Report of Investigations 7961

Tunnel Boring Technology

Disk Cutter Experiments in Metamorphic and Igneous Rocks

By Roger J. Morrell and David A. Larson
Twin Cities Mining Research Center, Twin Cities, Minn.

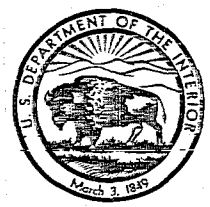

UNITED STATES DEPARTMENT OF THE INTERIOR
Rogers C. B. Morton, Secretary

BUREAU OF MINES
Thomas V. Falkie, Director

This publication has been cataloged as follows:

Morrell, Roger J

Tunnel boring technology: disk cutter experiments in metamorphic and igneous rocks, by Roger J. Morrell and David A. Larson. [Washington] U.S. Bureau of Mines [1974]

50 p. illus., tables. (U.S. Bureau of Mines. Report of investigations 7961)

Includes bibliography.

1. Tunneling. 2. Tunneling—Equipment and supplies. 3. Mining machinery. I. U.S. Bureau of Mines. II. Larson, David A., jt. auth. III. Title. IV. Title: Disk cutter experiments. (Series)

TN23.U7 no. 7961 622.06173

U.S. Dept. of the Int. Library

CONTENTS

ILLUSTRATIONS

ILLUSTRATIONS--Continued

TABLES

TUNNEL BORING TECHNOLOGY

Disk Cutter Experiments in Metamorphic and Igneous Rocks

by

Roger J. Morrell [1] and David A. Larson [1]

ABSTRACT

Bureau of Mines laboratory experiments with reduced scale cutter and cutter forces were performed to (1) define the fundamental relationships governing disk cutter performance and (2) to develop a method of predicting disk cutter performance in soft, medium, and hard rocks.

The rock cutting experiments were performed in four igneous and metamorphic rocks that ranged in compressive strength from 38,000 to 67,000 psi. A special testing machine called a linear cutter apparatus (LCA) was used to load and traverse a free rolling disk cutter across a smooth rock surface. Each pass of the disk produced a single crater, and runs were spaced to avoid breakage between craters. During each run the normal and tangential cutter forces were measured and recorded. The soft and medium rock data were obtained from previous Bureau experiments with disk cutters.

Crater depth, tangential cutter force, crater volume, specific energy versus normal cutter force, and crater width versus depth are defined within this study. With the use of standard physical properties, performance prediction equations were developed using stepwise linear regression analysis techniques. A method of using these prediction equations to calculate the boring rate, the cutter spacing, and the torque and energy requirements of a full-scale boring machine was also developed.

INTRODUCTION

The use of tunnel boring machines, raise borers, and shaft drills for mechanically excavating raises, shafts, and tunnels has increased significantly in the last decade. The many advantages of continuous mechanical excavation, such as increased advance rate, hole stability, safety, and minimum overbreak have led to its use in new areas of application. Recent developments in combined storm and sewer tunnels to eliminate water pollution during storm runoff reflect the increased use of mechanical excavation equipment (1).[2]

[1] Mining engineer.

[2] Underlined numbers in parentheses refer to items in the list of references preceding the appendix.

One such project, the Chicagoland Deep Sewer Project, will alone require approximately 30 miles of conveyance tunnels and 18,000 ft of vertical shafts. Another area of increased usage is in underground mines for ventilation shafts, ore passes, haulageways, etc. Here the advantages of safety (especially for boring raises), the high advance rate, and the increased stability of the opening have made raise boring and to a lesser extent tunnel boring an established mining technique.

The recent Organization for Economic Cooperation and Development (OECD) Advisory Conference on Tunneling in its report on tunneling demand (4) indicates that a total of 188,000 miles of hard rock tunnels are expected to be built in the 18 OECD countries in the next decade. This represents a 450-percent increase in length over hard rock tunneling in the last decade. Demand for underground openings is expected to increase in the fields of mining, utilities, rapid transit, and novel underground structures.

To date, the state-of-the-art of machine boring is fairly well advanced in both soft and medium strength rock but remains poorly developed in hard rock. Mechanical excavation, excluding raise boring, is presently limited to nonabrasive rocks with uniaxial compressive strength of approximately 30,000 psi. This excludes many of the commonly found rocks, such as granite, basalt, schist, quartzite, etc. In abrasive rocks, the upper limit of boreability is less, probably between 20,000 and 30,000 psi compressive strength. Although machines are being used in harder and harder rocks, the use of machines in very hard rock has resulted in slow progress or even machine failure in the past. The primary difficulty in boring hard rock is in the rock disintegration process, which suffers badly because of excessive cutter and cutter bearing wear. The National Academy of Sciences Committee on Rapid Excavation (8) estimates that rock disintegration in hard rock is one-third to one-half of total excavation costs, and the rate of excavation is the factor that ultimately limits the rate of advance. From the magnitude of the expected tunnel demand in the next decade, it is apparent that any improvement in this area would have far-reaching effects. The committee calls for a reduction in the real cost of excavation of from 30 to 50 percent and for a 200- to 300-percent increase in the sustained rate of advance in both soft, medium, and hard rock.

To study these and other areas, the Bureau's Twin Cities Mining Research Center initiated a research program into the rock disintegration process in rapid excavation. This report is one of a series that deals with tunnel boring technology. The first report (7) investigated the disintegration process in soft and medium-hard rocks from 9,000 to 27,000 psi compressive strength and established the experimental techniques and identified the variables important in the mechanical excavation processes.

This report deals with disk cutting experiments in hard rock. The hard rock cutting experiments were performed with a 7-in-diam disk cutter with a 90° cutting edge that was traversed in a straight line across a smooth rock surface. Each pass of the cutter produced a single crater with no breakage between craters. In this paper, a crater is defined as a long V-shaped slot or groove. Vertical load was varied between 3,000 and 14,000 lb. The rocks

studied were two varieties of granite, one basalt, and one quartzite, and all were massive in character with no visible fractures or planes of weakness. The physical properties of these rocks are given later in this report.

The first objective of this research was to determine the following relationships: (1) Crater depth as a function of normal cutter force, (2) crater volume as a function of input energy, (3) crater volume as a function of normal cutter force, (4) crater depth as a function of crater width, and (5) normal cutter force as a function of tangential cutter force. These relationships further an understanding of rock cutting and can be used to estimate the potential excavation rate torque requirements, and the energy efficienty of a full-scale mechanical excavation system.

The second objective of this research was to develop performance prediction equations for disk cutters. The preduction equations were of a form determined by the relationships found in the fundamental studies and involved forces or energies and the physical properties of the rock. Prediction equations were developed to predict crater depth as a function of normal cutter force and rock properties, crater volume as a function of input energy and rock properties, and tangential cutter force as a function of normal cutter force and rock properties. One series of these prediction equations was developed for the four hard rocks investigated in this report, and a second series was developed for both the hard and soft rocks. The soft rock data were from a previous report of investigations (7).

Previous related work by other researchers include that done by Rad (9), Hustrulid (3), Gaye (2), and Takaoka (11).

Work by Rad involved studies of disk cutters and heat assisted fragmentation. The primary objective of this work was to assess the effect of laser irradiation on the efficiency of rock cutting. In this work, the improvement in the efficiency of rock cutting was studied as a function of total heat input, input heat rate, cutter diameter, cutter thrust, cutter speed, and geometry of cutting. The primary results of this work are that heat assisted rock breakage is more efficient than unassisted breakage but that the additional cost of the heat is not commensurate with the improvement noted and that an optimum spacing exists for adjacent cutters where the volume of materail excavated is a maximum. This optimum spacing differs for different combinations of cutter diameter, cutter load, and rock type. One result directly comparable with the work covered by this report is that the higher cutter loads are more efficient for breaking rock than are the lower cutter loads in terms of volume of material excavated and minimum specific energy.

Work by Hustrulid (3) involved testing with small disk cutters as a method of predicting the performance of a full-scale machine. The equipment used for these tests was a modified milling machine that required the depth of cut to be fixed and the rock to be moved under the cutter. The maximum cutter force was 3,000 lb, which was necessitated by the small rock cores used in this work. A major conclusion of this work was that it was not possible to predict the performance of a full-size machine by using small disk cutters on rock cores. The authors believe that linear cutter tests can be used to

predict the performance of full-scale machines if the forces, cutters, and other experimental laboratory conditions more closely simulate real field conditions. The Bureau is currently conducting a research program to predict field performance using linear cutter-type tests, but results are not yet available.

Gaye (2) has recently advocated the use of a rock index number to predict the performance of a full-size machine. This number is defined as the unconfined compressive strength of the rock divided by the specific energy obtained with a boring machine. Specific energy is defined as the energy required to excavate a unit volume of rock. The authors feel that this parameter will be useful if specific energy can be determined prior to boring.

The work by Tokaoka (11) is the most closely related to the Bureau's work. The experimental setup procedures and cutter geometry were similar but the normal cutter loads were substantially less, being about 6,000 lb maximum. Maximum cutter load in the Bureau's experiment was 14,000 lb, and it was found that a cutter force of at least 8,000 lb was necessary to reduce the specific energy to a relatively constant value. However, the results that can be directly compared are as follows: (1) Depth of cut increases at a decreasing rate with increasing normal cutter force. This result does not agree with the linear or increasing rate of change relationships found between cutter force and depth of cut in the Bureau's work. (2) The tangential cutter force was found to increase at an increasing rate with normal cutter force, and the ratio of the tangential and normal force was approximately 0.10. (3) The sharper the cutting edge, the deeper the cut and the more tangential force produced. The results of 2 and 3 are in agreement with the Bureau's work.

The Bureau's work differs from the previously cited works in several important areas. First, the cutter diameter used (7 in) and the cutter loads used (maximum of 14,000 lb) were more closely related to field boring conditions; second, a greater number (a total of 9) and variety of rocks were tested including limestone, dolomite, marble, granite, basalt, and quartzite; and third, the Bureau's work is unique in attempting to predict disk cutter performance using a single standard rock property or a combination of standard rock physical properties. The results, which are promising, show that two properties, Shore scleroscope hardness and rock density, are the most often used although five other properties including Young's modulus, compressive strength, tensile strength, and shear modulus are also used.

EQUIPMENT

The rock cutter used in these experiments was a specially designed steel disk with a tungsten carbide cutting edge (fig. 1). The disk was 7 in. in diameter, 1 in. thick, and had a cutting edge angle of 90°. The cutting edge of the disk was constructed of 36 tungsten carbide inserts that were soldered around the periphery to form a continuous smooth cutting edge. The tip of the cutting edge was finished off with a small radius to minimize breakage and wear, and a single cutter was successfully used for all of the hard rock experiments with little apparent damage.

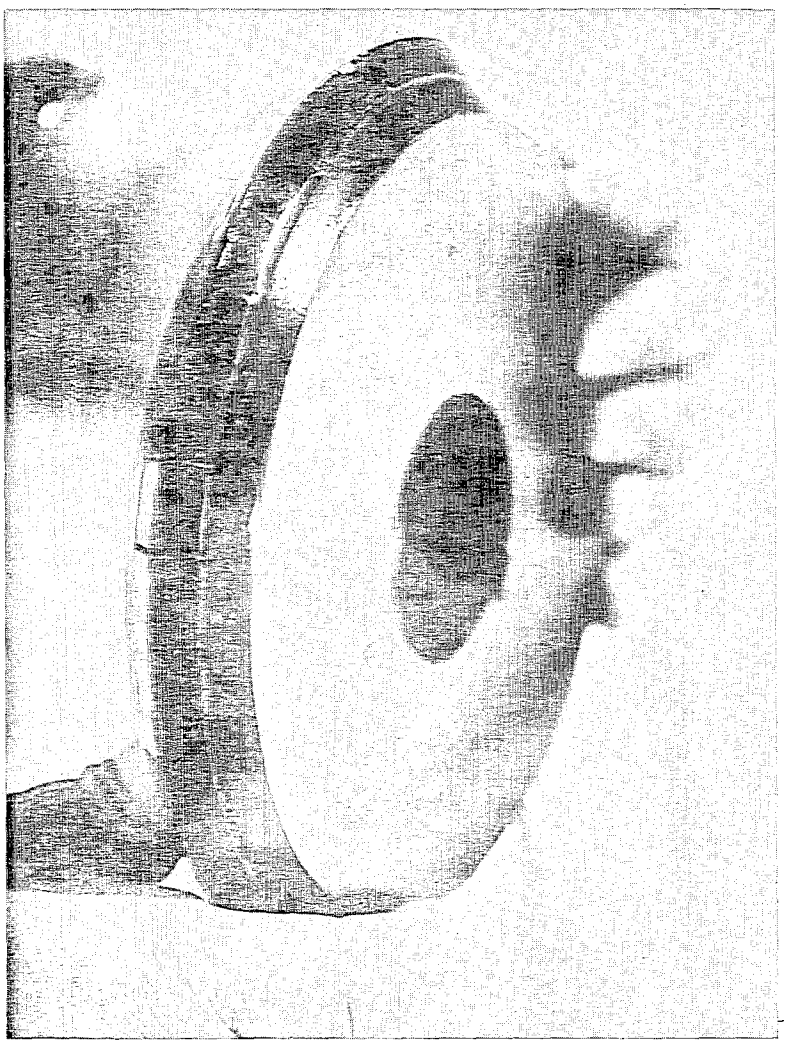

FIGURE 1. - Disk cutter with tungsten carbide cutting edge.

The disk cutter was mounted on a Bureau-designed testing machine (fig. 2) called a linear cutter apparatus (LCA). This apparatus was designed to load and traverse a rolling disk across the surface of a rock and to measure the forces acting on the cutter. The normal load and horizontal motion of the disk were provided by two hydraulic cylinders. The forces acting on the disk were measured with strain-gage load transducers, and the distance traveled was obtained from a 10-turn potentiometer. The output of the load transducers was simultaneously recorded as a function of the distance traveled as shown schematically in figure 3. A more detailed description of the equipment used during these experiments is given in the first report (7, pp. 3-5).

PROCEDURE

Operation

The rock specimen under test was placed on the rock platform located directly under the disk cutter. The height of the platform was adjusted so that when the disk was loaded down and penetrated into the rock, the yoke attached to the cutter shaft assembly would be level. This procedure insured that the load transducer mounted on the yoke would measure only the horizontal force component acting on the cutter. The rock was then laterally positioned to avoid interference with craters from previous runs and locked in place.

The cutter was loaded near one end of the rock, and the normal force was adjusted to the desired level. With the normal load preset, the cut was begun with the horizontal velocity held constant to 3 ips during all of these experiments. At the end of the run, usually about 20 in, the disk was unloaded.

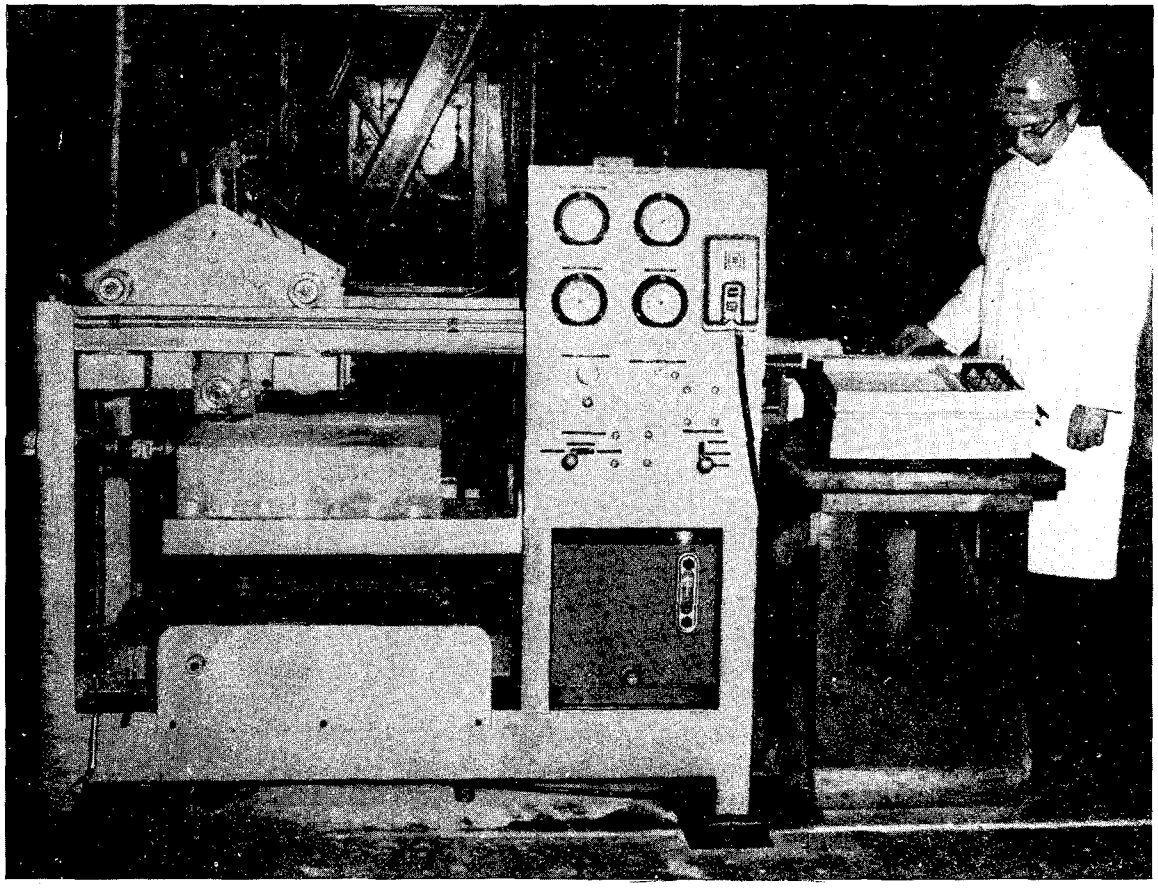

FIGURE 2. - Linear cutter apparatus.

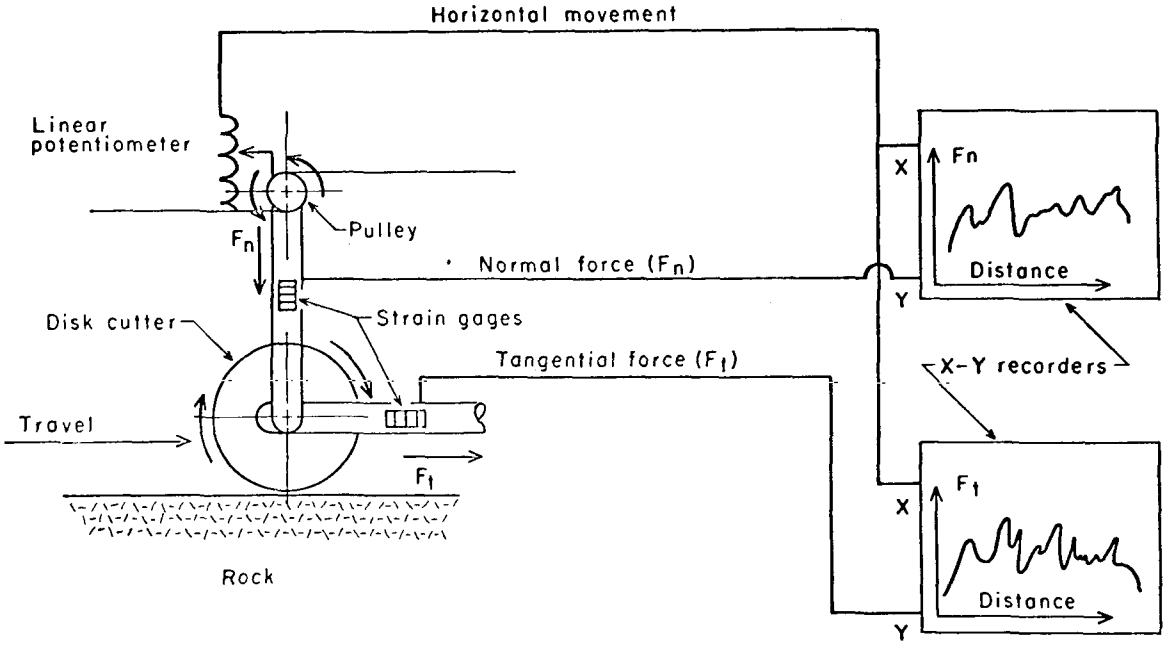

FIGURE 3. - Instrumentation schematic diagram for linear cutter apparatus.

Collection of Data

The traces of the normal and tangential forces recorded during the run were later analyzed to obtain the average forces acting on the cutter. This was accomplished by measuring the area under the force curves with a planimeter and dividing this area by the distance traveled by the cutter. The balance of the raw data was obtained from crater measurements. The width and depth of the crater, measured with a scale and micrometer probe, respectively, were taken at the same 1-in intervals along the length of the crater. The volume of the crater was calculated by dividing the weight of the chips created during the run by the density of the rock. Physical properties of all rocks utilized are presented in table 1.

TABLE 1. - Physical properties of rocks tested

Geologic name.....	Lac du Bonnet Quartz Monzonite	St. Cloud Gray Granodiorite	- - -	Sioux Quartzite
Commercial name.....	Lac du Bonnet granite	Charcoal granite	Dresser basalt	Jasper quartzite
Rock type.....	Quartz monzonite	Hornblende-biotite granodiorite	Basalt	Quartzite
Locality.....	Lac du Bonnet Manitoba, Canada	St. Cloud, Minn.	Dresser, Wis.	Jasper, Minn.
Compressive strength...psi..	38,300	39,110	63,610	67,470
Tensile strength.....psi..	1,133	1,376	1,982	2,057
Shore hardness scleroscope units..	95.6	95.9	85.8	105.7
Apparent density slugs/ft^3..	5.091	5.266	5.879	5.117
Apparent density.....g/cm^3..	2.624	2.714	3.029	2.637
Static Young's modulus 10^6 psi..	8.069	7.748	14.25	10.63
Longitudinal velocity..fps..	15,951	18,838	21,873	17,254
Bar velocity.....fps..	14,255	17,231	19,514	16,988
Shear velocity.....fps..	9,895	11,119	12,264	11,821
Dynamic Young's modulus 10^6 psi..	7.18	10.86	15.54	10.25
Poisson's ratio.....	0.2706	0.2479	0.2725	0.1152
Shear modulus.....10^6 psi..	3.46	4.52	6.14	4.96

Data Analysis

Curve fitting of the data throughout this report was done using regression analysis techniques. A special computer program using regression analysis was developed at the Twin Cities Mining Research Center and was capable of choosing the best statistical fit of six equation types: Linear, exponential, power, and three variations of the hyperbolic curve. The best

equation type is selected by choosing the largest percent explained variance. The standard error of estimate is determined by

$$S_e = \left[\sum_{i=1}^{n} (y_i - \hat{y}_i)^2/(n-2) \right]^{\frac{1}{2}}, \quad (1)$$

where S_e = standard error estimate,

n = number of observations,

y_i = i^{th} observation,

and $\hat{y}_i$ = estimate of the equation of regression line (5-6).

The technique used to develop the predictor equations shown in this report was a stepwise linear regression analysis. This program type can be found within the statistical library available with any computer system. The statistical regression model was derived as follows:

$$\hat{Y} = \hat{\beta}_o + X^{\alpha} \left(\frac{\hat{\beta}_1}{RP_1} + \frac{\hat{\beta}_2}{RP_2} + \ldots + \frac{\hat{\beta}_n}{RP_n} \right), \quad (2)$$

where $\hat{Y}$ = dependent variable to be estimated (either crater depth, crater width, crater volume, or tangential cutter force),

X = an independent variable (either normal cutter force, input energy, or crater depth),

α = optimum exponent,

$\hat{\beta}_i$ = the desired regression coefficients from the regression analysis,

and RP_i = independent variables (selected physical properties of the rock).

The stepwise regression procedure is to first select the physical property that accounts for most of the variance in the data. The procedure is repeated by adding the next most significant physical property, one at a time, until the predication equation cannot be further improved. F-testing at the 99.5-percent level was performed to determine whether or not a particular regression coefficient was significant. If the test showed the coefficient to be insignificant it was dropped from the equation.

RESULTS OF LINEAR CUTTER EXPERIMENTS WITH DISK CUTTERS

Typical Craters

Figure 4 shows a number of test craters typical of those created during the disk cutter experiments. These craters were formed by a disk cutter with a 90° cutting edge in a test block of limestone. The illustrated craters, approximately 21 in long, 0.3 to 2 in wide, and 0.1 to 0.5 in deep, were formed with vertical loads of from 3,000 to 9,600 lb.

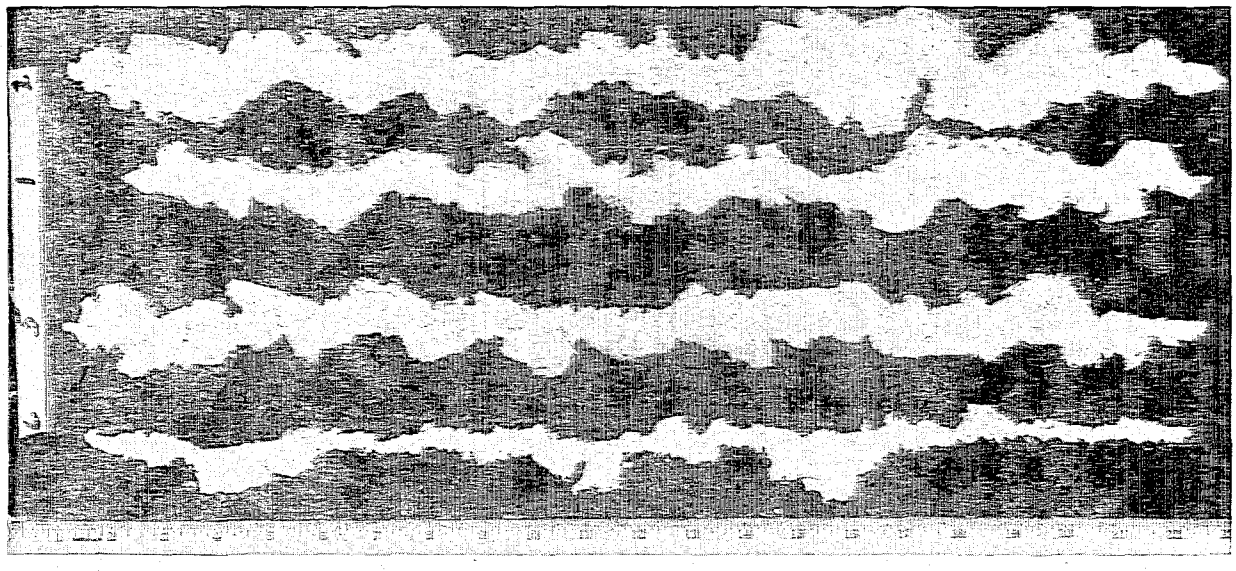

FIGURE 4. - Typical craters produced during disk cutting.

Crater Depth as a Function of Normal Force on the Cutter

The normal cutter force was defined as the average normal force acting on the cutter over the length of a run. This procedure was necessary since the cutter forces varied considerably about the preset cutter load. Typically, peak cutter forces (both normal and tangential) were 10 to 80 percent larger than the average cutter force. The crater depth was similarly defined as the average cutter depth as measured at 1-in intervals along the crater.

The crater depth versus normal cutter force relationships for the four hard rock tested are shown in figure 5. The normal cutter force is plotted as the independent variable and the crater depth as the dependent variable. Table 2 shows the best-fit equation for these curves. The equation that best represented all of the crater depth versus normal force relationships was

$$D = KF_n^{x}, \tag{3}$$

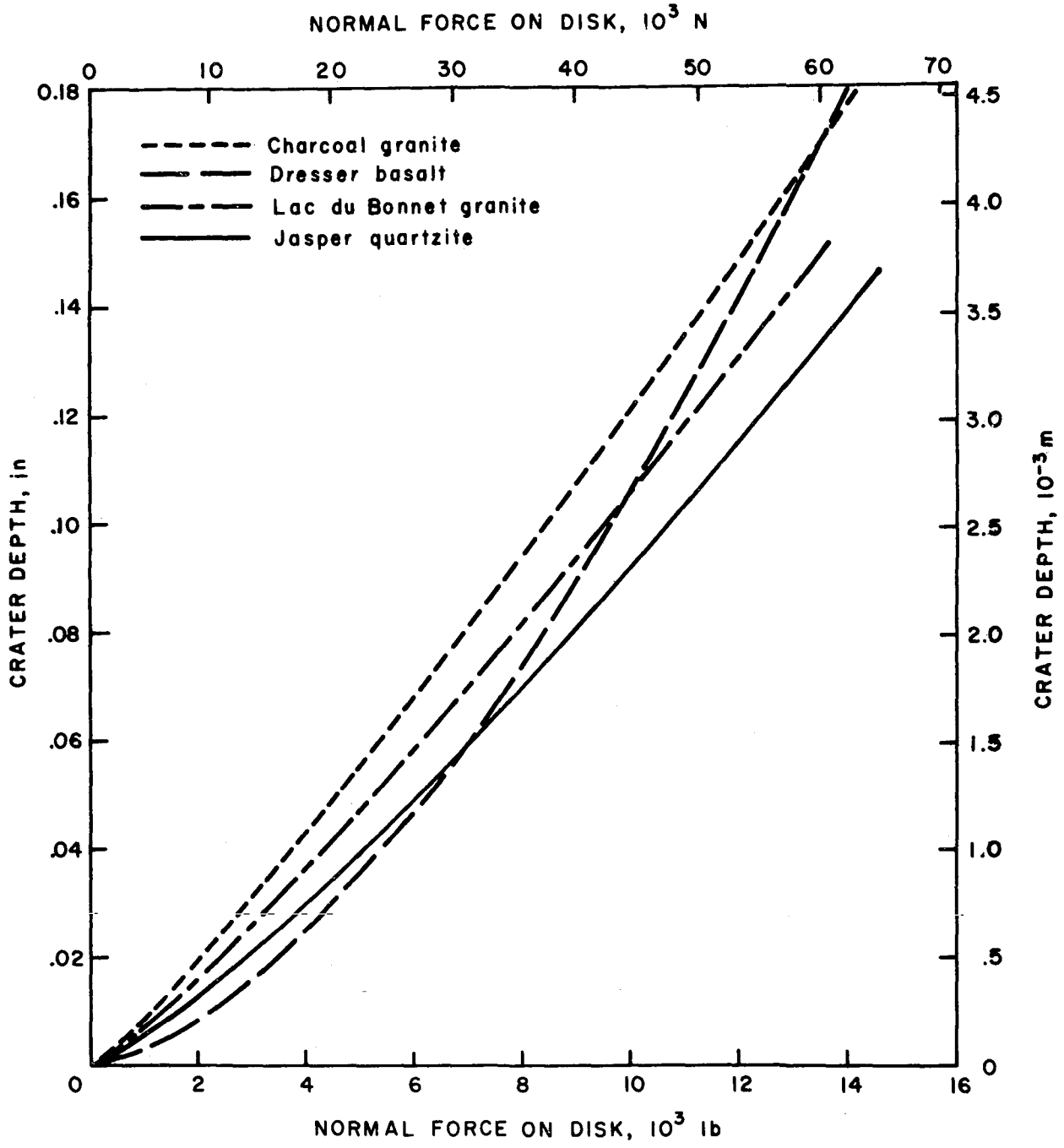

FIGURE 5. - Crater depth as a function of normal cutter force.

where D = crater depth, inches,

K = a constant depending on rock properties,

F_n = a normal cutter force, pounds,

and x = an exponent that differs for each rock.

Note from table 2 that in all but one rock, the crater depth varies as a function of the normal cutter force raised to a power between 1.1 and 1.2. This result differs slightly from previous experiments in soft rocks where the crater depth varied linearly with normal force. No explanation for this behavior is given except to note that the second group of rocks tested were considerably harder and more dense than the first. An inspection of the physical properties in table 1 and table 3 shows significant differences in compressive strength, Shore scleroscope hardness, density, and static Young's modulus.

TABLE 2. - Crater depth as a function of normal force[1]

Rock type	Crater depth, in, as a function of normal force, lb	S_e[3]
Lac du Bonnet granite.....	$D = 2.48 \times 10^{-6} F_n^{1.16}$	0.006
Charcoal granite.....	$D = 3.49 \times 10^{-6} F_n^{1.14}$	.006
Dresser basalt.....	$D = 4.63 \times 10^{-6} F_n^{1.59}$	.002
Jasper quartzite.....	$D = 1.08 \times 10^{-6} F_n^{1.23}$	.004

[1]The computer determined equations in the table and equations 4 and 5 are accurate to two significant figures.

[2]The standard error of estimate is calculated as follows:

$$S_e = \left[\frac{1}{n-2} \sum_{i=1}^{n} (y_i - \hat{y}_i)^2 \right]^{1/2}.$$

This statistic is analogous to the standard deviation that measures the variation of a set of data from a mean value. The standard error of estimate measures the variation between observed values and calculated values. The larger the standard error of estimate, therefore, the greater the scatter in the data. With S_e known, a confidence interval for $\hat{y}_i$ can be calculated for any value of x_i using standard formulas given in any statistics work (5-6).

TABLE 3. - Physical properties of soft and medium strength rocks[1]

...logic name.....	Salem Limestone	Salem Limestone	Oneota Member Prairie du Chien Formation	Holston Limestone	Cordell Dolomite Member, Mamistique Formation
...rcial name.....	Indiana limestone, type 2	Indiana limestone, type 1	Kasota stone	Tennessee marble	Valders white rock
...lity.....	Bedford, Ind.	Bedford, Ind.	Kasota, Minn.	Knoxville, Tenn.	Valders, Wis.
...pressive strength.....psi..	9,126	9,991	13,184	16,809	27,230
...sile strength.....psi..	679	502	792	1,219	793
... hardness..scleroscope units..	27	32	37	55	68
...ent density.....slugs/ft^3..	4.455	4.635	4.818	5.186	5.056
...ent density.....g/cm^3..	2.302	2.395	2.487	2.681	2.613
...ic Young's modulus....10^6 psi..	3.5	4.4	5.7	9.0	5.7
...gitudinal velocity.....fps..	14,570	14,610	17,119	20,058	12,815
... velocity.....fps..	13,062	12,007	14,708	16,845	12,118
...r velocity.....fps..	11,482	8,489	9,360	10,590	8,513
... Young's modulus...10^6 psi..	5.29	4.65	7.42	10.29	5.17
...sson's ratio.....	0.27	0.33	0.28	0.32	0.20
... modulus.....10^6 psi..	2.09	2.32	2.90	4.07	2.55

From reference 7, page 7.

To determine the crater depth or depth of penetration for a disk cutter in rocks other than those tested (but with approximately the same physical properties), a prediction equation was developed. The procedure used was a stepwise multiple linear regression. This procedure entered one independent variable at a time to give a series of equations each containing one more independent variable than the equation preceding it. F-testing at the 99.5-percent level was used to determine the significance of the regression coefficients found during the regression analysis. To determine the optimum exponent for the prediction equation, an iterative procedure was used. This process was performed until a maximum multiple correlation coefficient and a minimum standard error of estimate were found. From the fundamental relation to be fitted, the following prediction equation was developed:

$$D = 0.004 + F_n^{1.2} \left(\frac{1.25 \times 10^{-4}}{SH} + \frac{3.50}{E_s} \right), \qquad (4)$$

where D = estimated crater depth, inches,

F_n = normal cutter force, pounds,

SH = Shore scleroscope hardness, scleroscope units,

and E_s = static Young's modulus, pounds per square inch.

Equation 4 had a multiple correlation coefficient of 0.957 and a standard error of estimate of 0.013 in. Prediction equation 4 and all prediction equations shown in this report are valid for all rocks whose properties fall within the range of the physical properties of the rocks used to calculate it. For example, predictor equation 4, which used Shore hardness and static Young's modulus, is assumed to be valid for any rock whose values of Shore hardness and Young's modulus fall within the range of the rocks used to calculate it, irrespective of any other physical properties. Equation 4 is therefore valid for rocks with a Shore hardness between 85 and 105 and a Young's modulus between 7.7×10^6 psi and 14×10^6 psi.

Note that equation 4 is of the form $y = ax^b$ and identical to the form of the best-fit equations in table 2 except for the constant 0.004, which can be dropped from the equation without any serious loss of accuracy. Equation 4 is derived from the equations in table 2, with the constant in the table 2 equations replaced by the terms inside the brackets in equation 4. The terms in brackets represent the effect of rock, since all other conditions were constant. The reciprocals of the rock properties were used instead of the untransformed properties since this transformation causes a logical decrease in crater depth as SH and E_s become larger. A high value of Shore hardness and Young's modulus is synonymous with harder rocks. One other variable, shear modulus, was found significant at an F-level of 99.5 percent but was not included in the equation since it did not significantly increase the accuracy.

To demonstrate the accuracy of this equation, a plot of the actual crater depths and the predicted values are shown in figure 6. The predicted values are in all cases within 8 percent of the real values and in most cases are

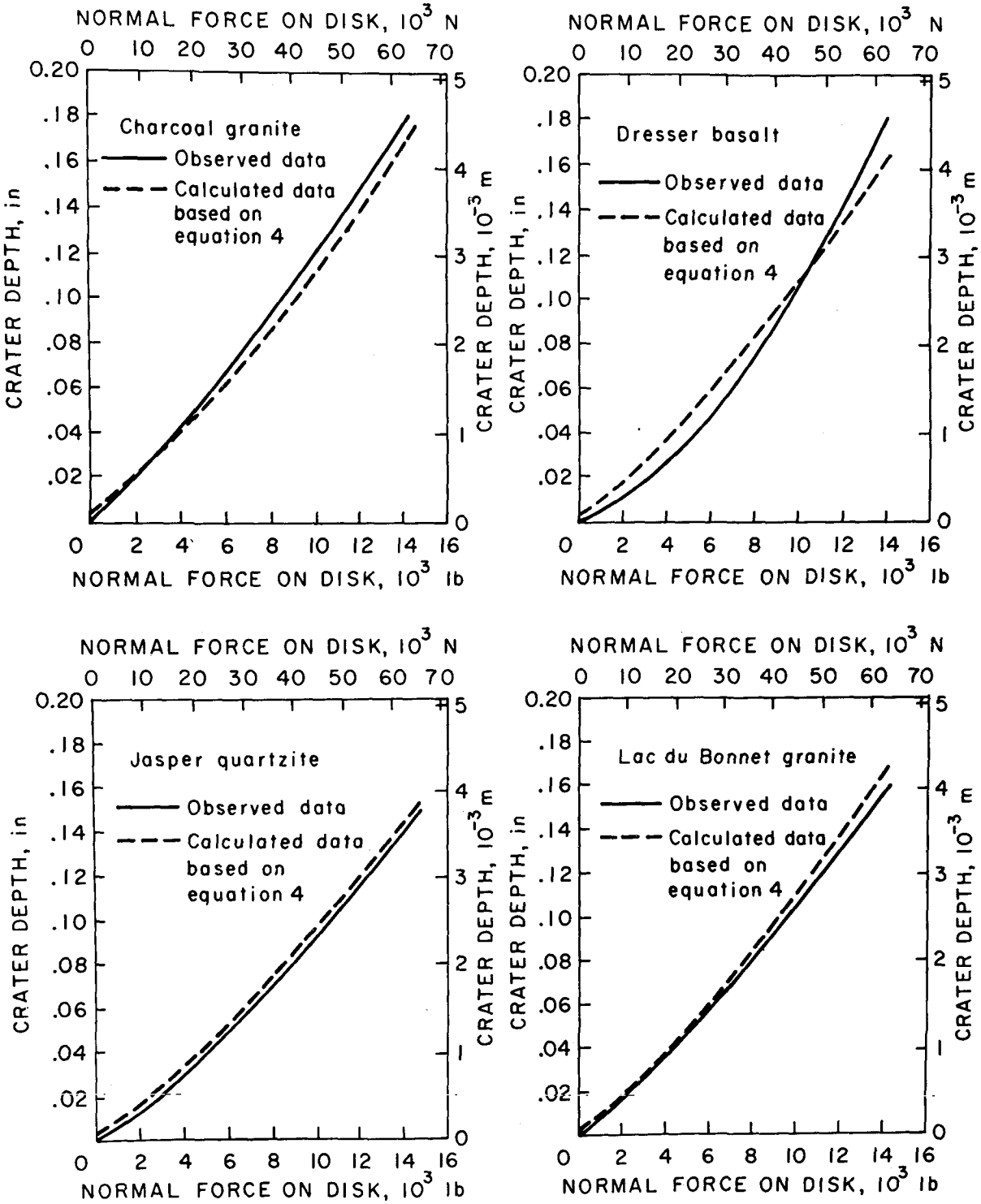

FIGURE 6. - Actual crater depth versus predicted crater depth (from equation 4) for hard rocks.

between 2 and 6 percent. The reader is cautioned that the accuracy of the prediction equations developed in this report have not yet been verified for rocks other than those shown in this report. Equation 4 can be used to estimate crater depth (and therefore penetration) for rocks other than those tested if their physical properties fall within the range of those tested.

Although equation 4 can be used to predict crater depth for hard rocks, another predictor equation was developed that is applicable to both soft, medium, and hard rocks. The soft rock data were obtained in previous Bureau work and the physical properties of these rocks are shown in table 3. The following equation can be used for rocks with a Shore hardness, SH, of between 27 and 105 that have densities, P, of 2.3 and 3.0 g/cm^3, and a static Young's modulus, YM_s, of between 3.5 X 10^6 and 14.2 X 10^6 psi:

$$D_{90} = -0.006 + F_n \left(\frac{3.26 \times 10^{-4}}{SH} + \frac{1.75 \times 10^{-5}}{P} + \frac{13.92}{YM_s}\right). \quad (5)$$

Equation 5 has a multiple correlation coefficient of 0.953 and a standard error of estimate of 0.014 in. The accuracy of this equation is shown in figures 7-8. In all instances, the predicted depth is within 7 percent of the observed value.

Equations 4-5 are valid only for disk cutters with a 90° cutting edge. To correct this value for cutters with a 60° cutting edge, multiply the depth by 1.69 as shown:

$$D_{60} = 1.69\ D_{90} \quad (7, \text{ p. } 29). \quad (6)$$

A study of the relationship between crater depth and normal cutter force has the following practical applications: First, the nearly linear nature of the crater depth-normal force equations (exponent varies from 1.0 to 1.5) shows that any increase in the thrust on a boring machine should result in a nearly proportional increase in the depth that the individual cutters penetrate into the rock face. This is affirmed by related work at the Bureau's Twin Cities Mining Research Center involving the drilling of 24-in-diam holes using full-size boring machine disk cutters. In this work (not yet published), the penetration rate was found to increase at an increasing rate with increasing thrust. Therefore, it would be expected that the penetration rate of a mechanical mole would increase either in direct proportion to or at an increasing rate with an increase in cutting force. The second practical application of the laboratory results is that they allow a comparison to be made of the cutting characteristics of different rocks. For example, a rock with a large value of Shore scleroscope hardness and Young's modulus would be more difficult to bore than a rock with lower values of these properties. Rocks with approximately the same Shore hardness and Young's modulus should bore at approximately the same rate.

Note that the cutter geometry, thrust, rotary speed, and rock condition (blocky, massive, etc.), essentially would have to be identical for this

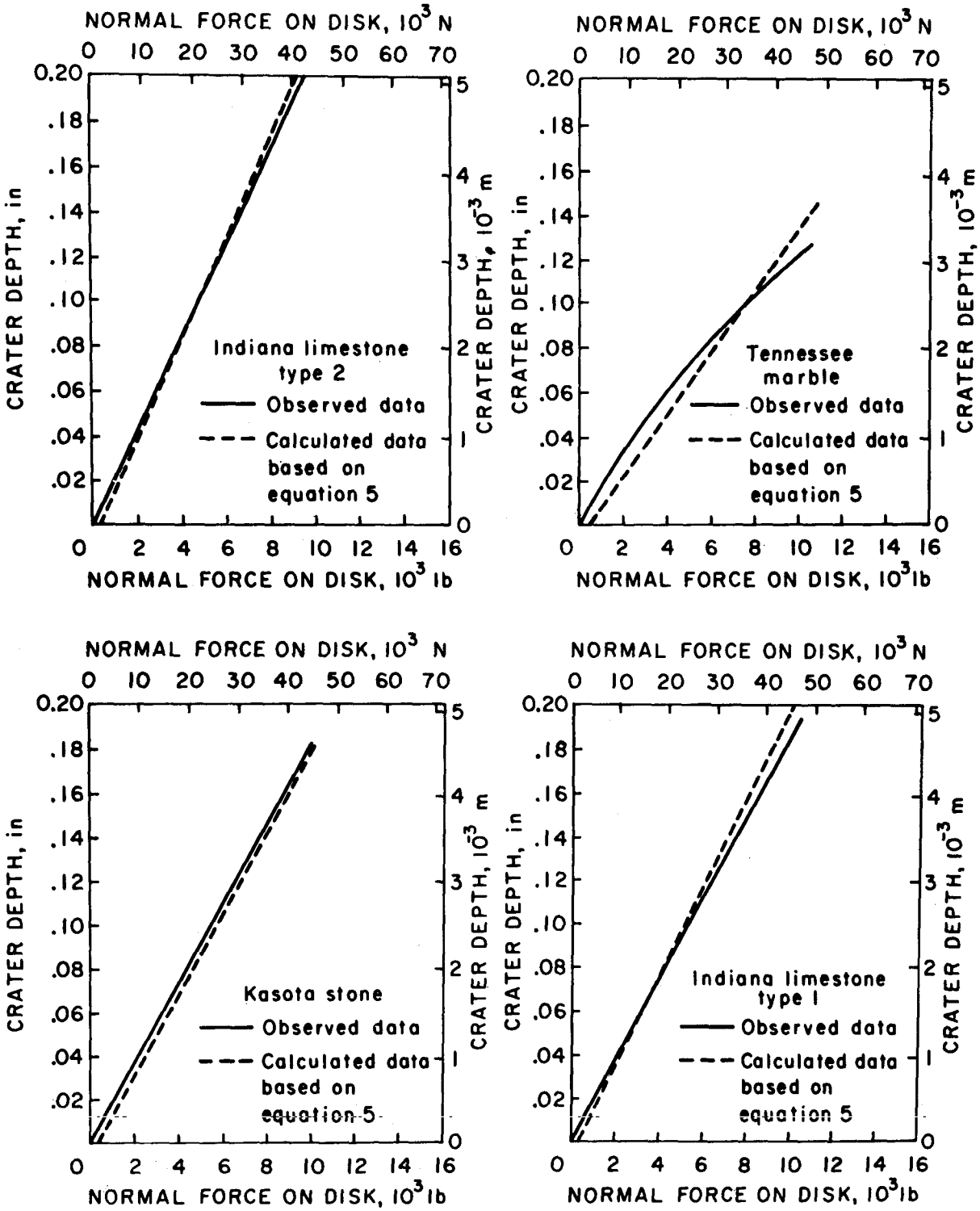

FIGURE 7. - Actual crater depth versus predicted crater depth (from equation 5) for soft and medium rocks.

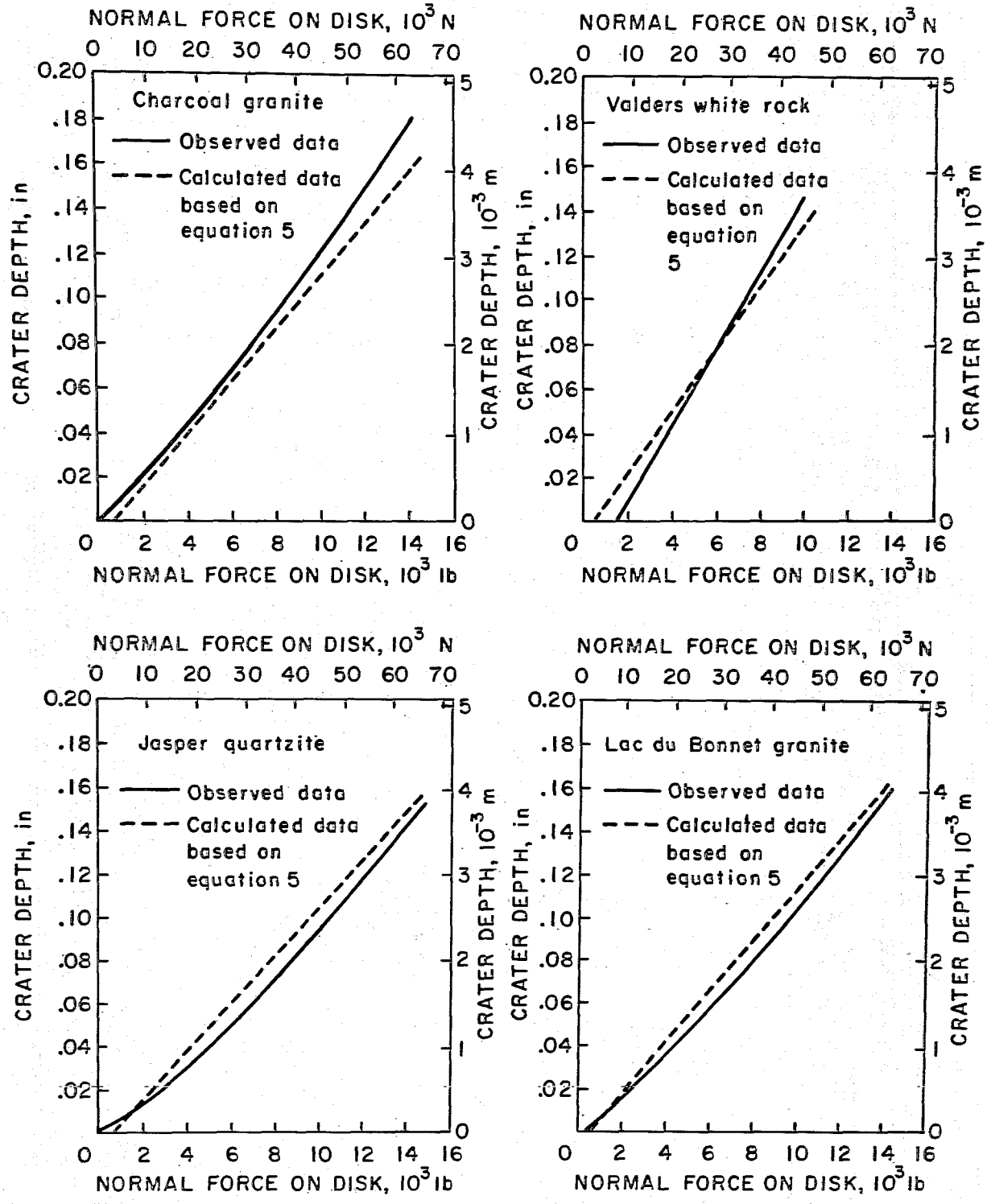

FIGURE 8. - Actual crater depth versus predicted crater depth (from equation 5) for medium and hard rocks.

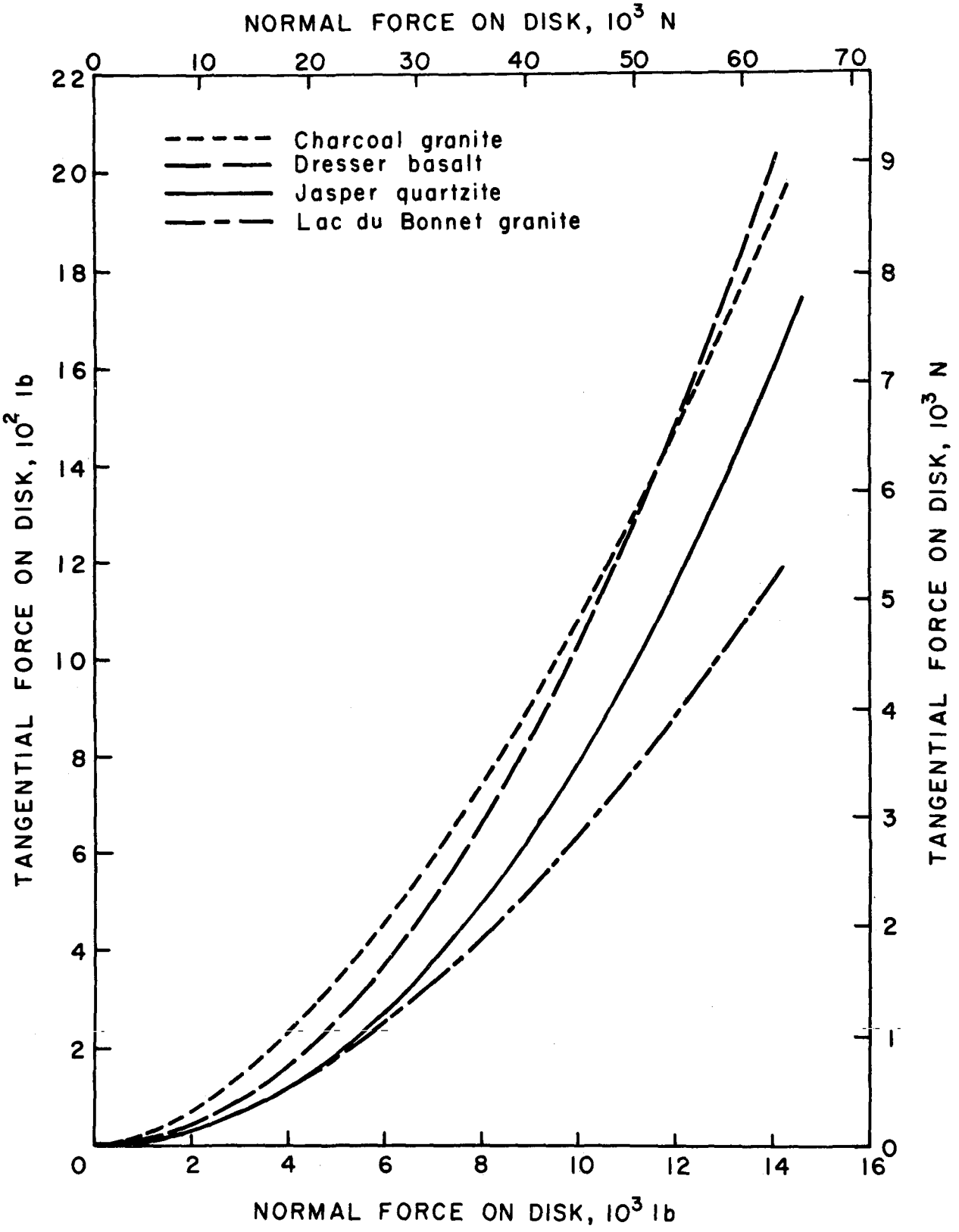

FIGURE 9. - Tangential cutter force as a function of normal cutter force.

comparison to be valid. With these limitations in mind, the potential boring rate of a mole could be predicted using a simple ratio as follows:

$$\frac{D_1}{D_2} = \frac{B_1}{B_2} \quad \text{(all conditions identical)}, \tag{7}$$

where D_1 = crater depth for rock 1 to be calculated from equation 4 for hard rocks or from equation 5 for soft, medium, and hard rocks,

D_2 = crater depth for rock 2 to be calculated from equation 4 or 5,

B_1 = instantaneous boring rate for rock 1 to be determined,

and B_2 = known instantaneous boring rate for rock 2.

The values of D_1 and D_2 would be calculated using the appropriate prediction equation. For hard rocks use equation 4, and for rocks other than hard, use the combined soft and hard equation (equation 5). The closer related the boring conditions are for rock 1 and rock 2, the more accurate will be the predicted boring rate (B_1).

Tangential Cutter Force as a Function of Normal Cutter Force

The tangential cutter force is the force required to roll the disk cutter across a rock surface and is the force that determines the torque required to rotate the cutterhead of a mechanical boring machine. Tangential cutter force is shown as a function of normal cutter force in figure 9. The equations of these curves are listed in table 4. The equation that best fits the data was, for all the rocks tested, as follows:

$$F_t = KF_n^x, \tag{8}$$

where F_t = tangential cutter force, pounds,

F_n = normal cutter force, pounds,

K = a constant that differs for each rock, pounds $^{(1 - x)}$,

and x = an exponent that ranged from 1.7 to 2.1.

The curves in figure 9, and the equations in table 4 show that the tangential cutter force increases approximately as the square of the normal force. To determine the ratio of the cutter forces (that is, coefficient of friction) the tangential force was calculated at a realistic normal force of 14,000 lb. The ratio of tangential and normal forces at this point for all the rocks was between 0.086 to 0.136, which compared closely with those obtained for disk cutters in soft rock (0.07 to 0.10). Note that the ratios are valid only for the discrete point at which they are calculated since tangential force increases at an increasing rate with normal force.

TABLE 4. - Tangential force as a function of normal force[1]

Rock type	Tangential force, lb, as a function of normal force, lb	S_e[2]
Lac du Bonnet granite.....	$F_t = 3.49 \times 10^{-5} F_n^{1.81}$	39.9
Charcoal granite.....	$F_t = 1.94 \times 10^{-4} F_n^{1.69}$	58.6
Dresser basalt.....	$F_t = 1.02 \times 10^{-5} F_n^{2.00}$	191.9
Jasper quartzite.....	$F_t = 3.63 \times 10^{-6} F_n^{2.08}$	56.5

[1]The computer determined equations in the table and equations 9 and 10 are accurate to two significant figures.
[2]Standard error of estimate.

It must be pointed out that the tangential cutter force obtained during these experiments was measured at the shaft of the cutter (fig. 3). Because of the mechanical configuration of the linear cutter, this measured tangential force is approximately 22 percent larger than the actual cutting force, which acts at the cutter-rock interface. Since the cutter force data were used only to define the fundamental relationships involved in disk cutting and to determine the effect of rock properties, the absolute value of this cutter force was of no consequence in this work. However, for those who require the absolute value of tangential force, this can be obtained by multiplying the tangential forces given in this report by 0.78.

To determine the tangential force acting on a 90° disk cutter for rocks other than those tested but with a Shore hardness between 85 and 105, a prediction equation was developed. The procedure used was stepwise multiple linear regression analysis with the value of the exponent determined by iteration. The best predictor equation developed was

$$F_t = -40.64 + F_n^{1.7} \left(\frac{0.014}{SH}\right). \tag{9}$$

Equation 9 had a multiple correlation coefficient of 0.932 and a standard error of 193.8 lb. Three other properties were found significant at the F-level of 99.5 but were eliminated from the equation because they made no improvement in the accuracy of the equation. The accuracy of this equation is shown in figure 10 as the dotted lines. Note that the average maximum error for all but one of the rocks tested was within 12 percent of the real value.

One other predictor equation for the tangential cutter force was derived during this study. This equation was developed to predict cutter force for both hard rock and soft rock. This equation can be used in rocks with a Shore hardness between 27 and 105 and with a density between 2.3 and 3.0 g/cm^3.

$$F_t = 40.6 + F_n^{1.9} \left(\frac{3.09 \times 10^{-4}}{SH} + \frac{4.64 \times 10^{-5}}{P}\right). \tag{10}$$

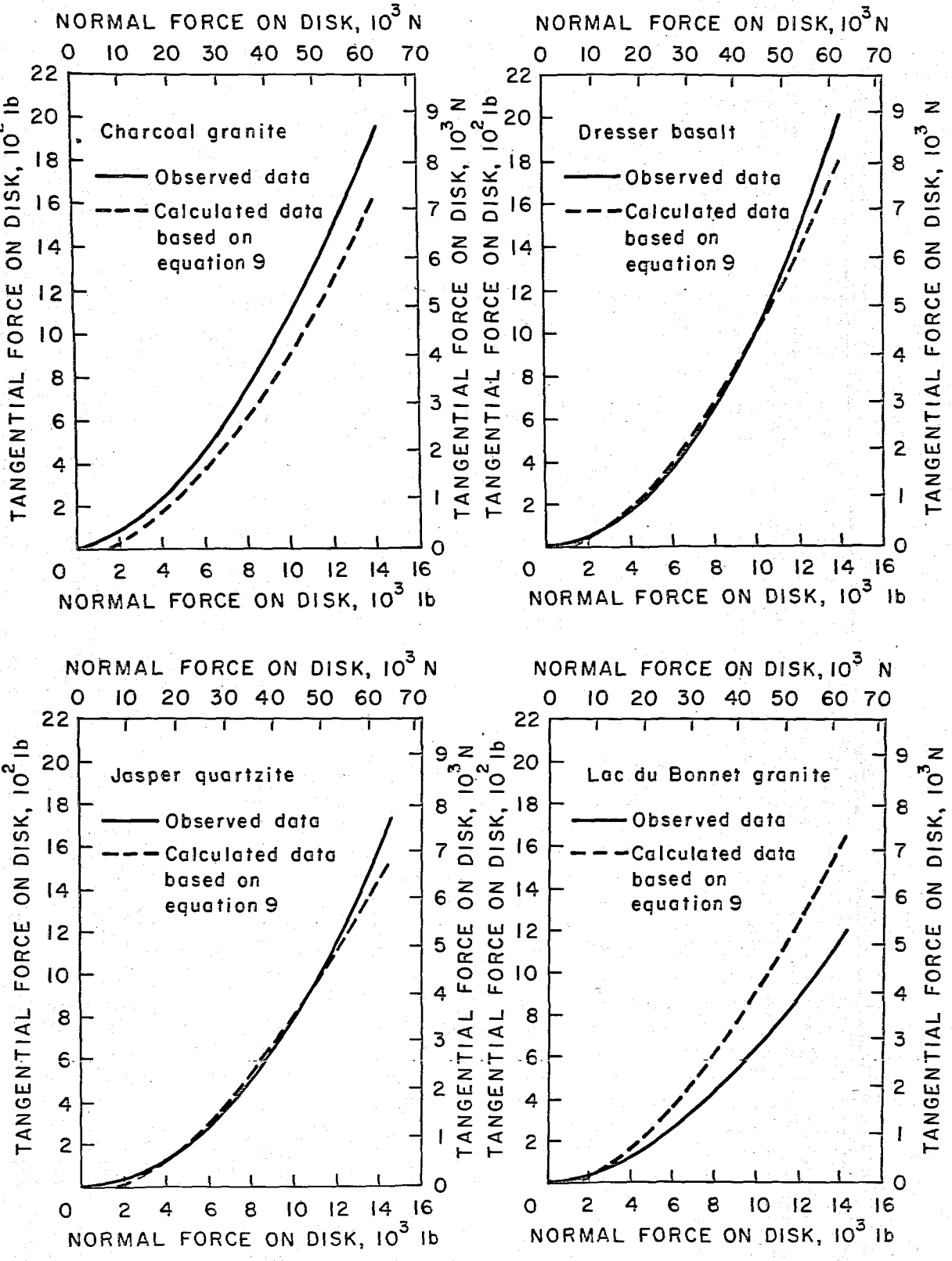

FIGURE 10. - Actual tangential cutter force versus predicted tangential cutter force (from equation 9) for hard rocks.

Equation 10 has a multiple correlation coefficient of 0.924 and a standard error of estimate of 186.9 lb. The accuracy of this equation is shown in figure 11-12. In most cases, the maximum error is less than 10 percent.

From previous work, it is also possible to modify the value of force obtained for the 90° cutting edge for a 60° cutting edge. The tangential force on the 60° cutter will be larger than the blunter 90° cutting edge as follows:

$$F_{t_{60}} = 1.46\ F_{t_{90}} . \tag{11}$$

Knowledge of tangential cutter forces is important in mechanical boring design since tangential cutter forces, along with cutter spacing, determine the torque required to rotate the boring machine cutterhead. The torque required to rotate the cutterhead is the sum of the tangential force acting on each individual cutter force times the torque arm measured from the center of the cutterhead to the individual cutters. This can be written as follows:

$$T = \sum_{i=1}^{n} F_{n_i} R_i , \tag{12}$$

where T = cutterhead torque, foot-pounds,

n = total number of cutters,

F_{n_i} = tangential cutter force acting on an individual cutters, pounds,

and R_i = distance from center of cutterhead to individual cutter, feet.

The absolute values of tangential forces determined in this work are not directly applicable to field use primarily because the cutter geometry and linear motion studied do not simulate field condition. However, they enhance the understanding of physical phenomenon and yield the following practical results: First it can generally be expected that tangential cutter force will continue to vary approximately as the square of the normal force and that rocks with large values of Shore scleroscope hardness will require less tangential force than rocks with low values of hardness. In more general terms, this means that the harder the rocks, the shallower the cutter penetration and the lower the tangential force required to roll the cutter across the rock. From previous experimentation it is also known that cutters with cutting edge angles lesser than 90° produce larger tangential forces and edge angles greater than 90° will require less force. In addition, for the same loading conditions, larger diameter cutters will require less tangential force than smaller diameter cutters. More experimentation is planned at the Bureau's Twin Cities Mining Research Center that will more closely simulate field conditions, the results of which will be directly applicable to full-size mechanical cutters.

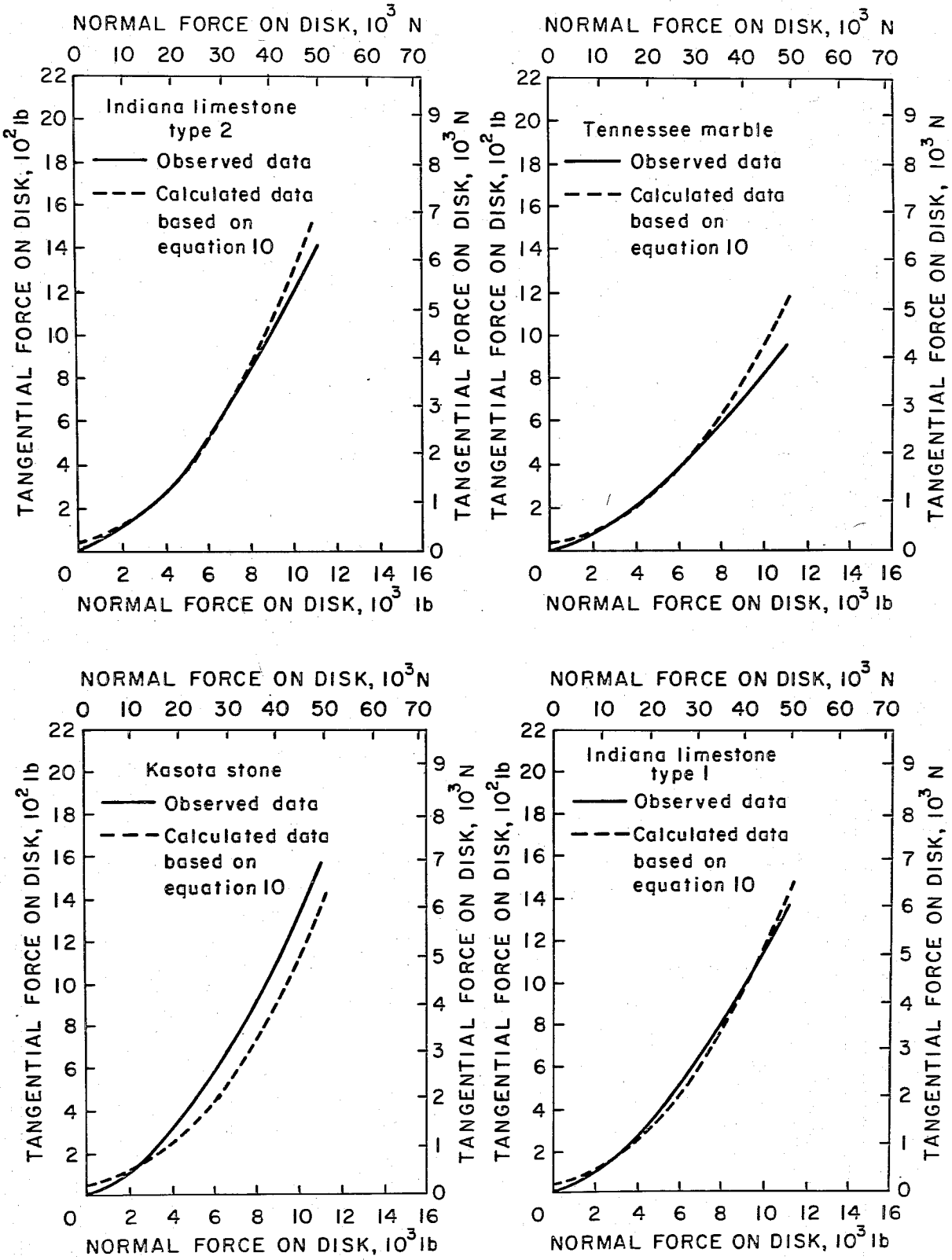

FIGURE 11. - Actual cutter force versus predicted tangential cutter force (from equation 10) for soft and medium rocks.

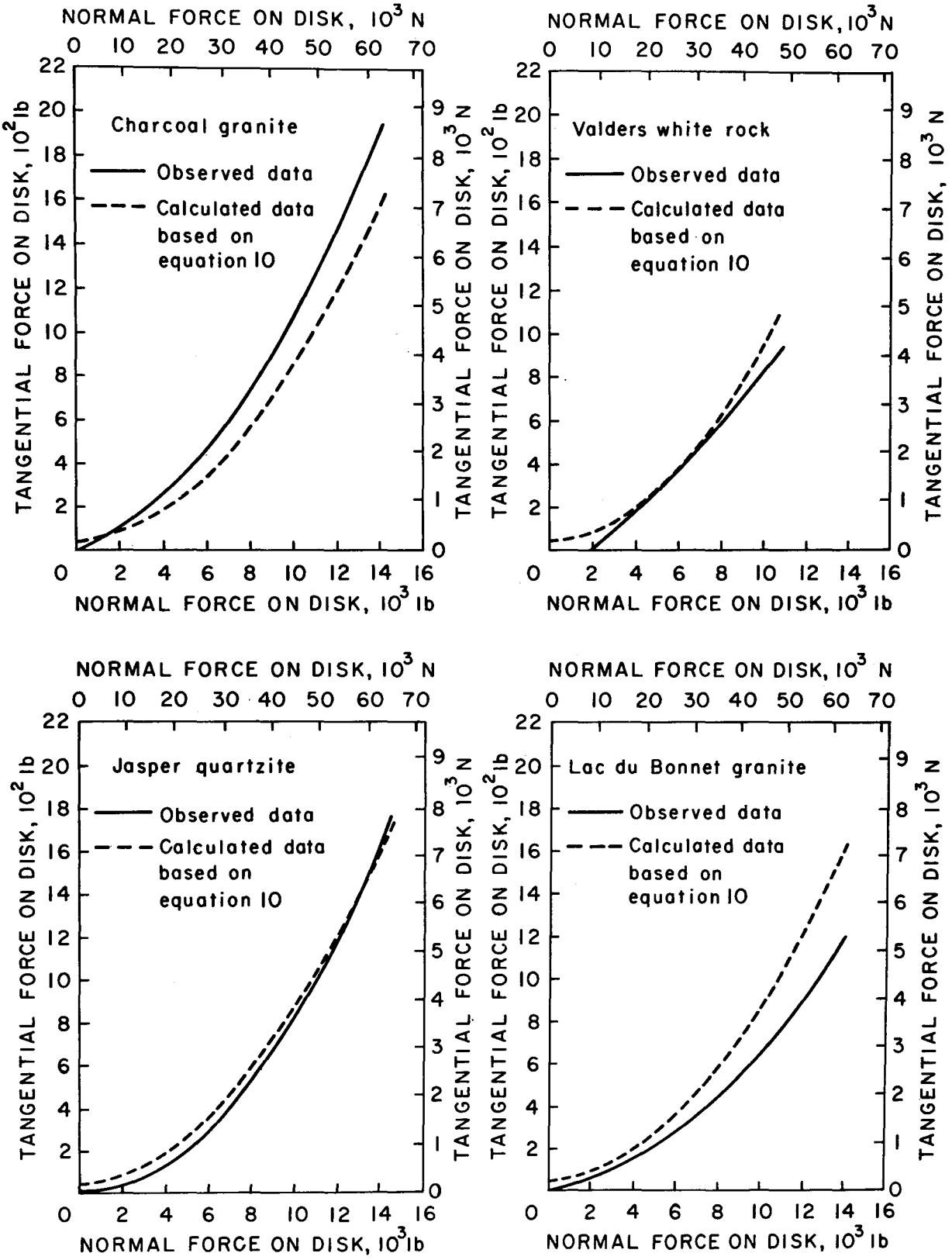

FIGURE 12. - Actual cutter force versus predicted tangential cutter force (from equation 10) for medium and hard rocks.

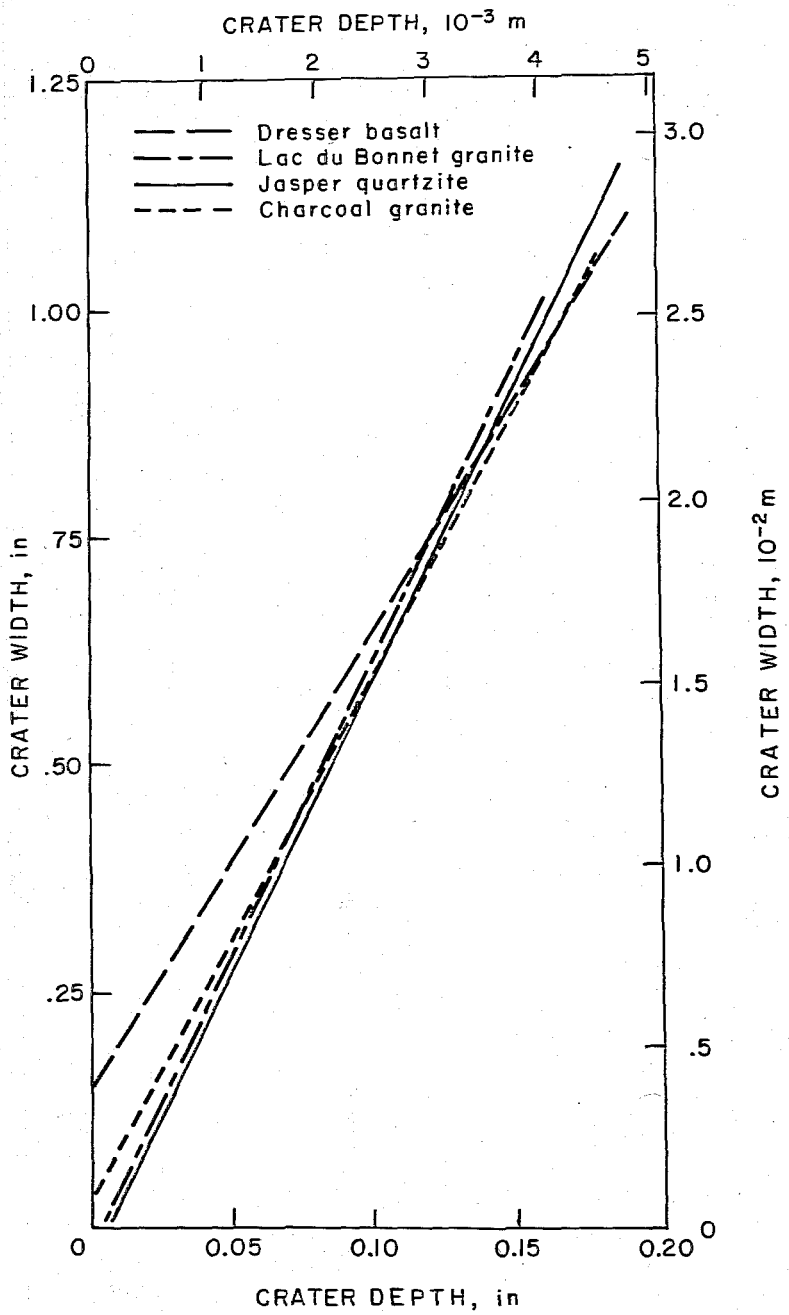

FIGURE 13. - Crater width as a function of crater depth.

Crater Width as a Function of Crater Depth

Crater width was defined as the average width of the crater as calculated from measurements taken at 1-in intervals along its entire length and crater depth as the average depth of the crater as calculated from measurements made at the same 1-in intervals along its entire length.

Figure 13 shows the crater width as a function of crater depth for all of the rocks rested. The crater depth is plotted as the independent variable, and crater width, as the dependent variable. The crater depth-crater width relation for all of rocks was found to be linear as shown in equation 13:

$$W = W_o + KD, \qquad (13)$$

where W = average crater width, inches,

W_o = intercept, inches,

K = the slope of straight line, inch per inch,

and D = average crater depth, inches.

The best-fit equations computed from the crater width and depth data for all the rocks tested are shown in table 5. The intercept, W_o, in equation 13, has no physical significance since it is not possible to produce a crater with a zero depth and a finite width or vice versa. Since in most cases the intercepts are small, they can be dropped from the equations without a significant loss of accuracy.

TABLE 5. - Crater width as a function of crater depth[1]

Rock type	Crater width, in, as a function of crater depth, in	S_e[2]
Lac du Bonnet granite.....	W = -0.03 + 6.50 D	0.047
Charcoal granite.....	W = 0.02 + 5.78 D	.052
Basalt.....	W = 0.13 + 5.09 D	.116
Jasper quartzite.....	W = -0.04 + 6.38 D	.037

[1]The computer determined equations in the table and equations 14 and 15 are accurate to two significant figures.
[2]Standard error of estimate.

The depth-width equations in table 5 shows two important results. First, the crater width is a linear function of the crater depth for all of the rocks tested. Second, the crater width is between five and six times the crater depth for all four rocks tested. This result shows that in spite of large differences in rock type and physical properties, except for Shore scleroscope hardness, the difference in crater width for the same crater depth is minimal for the rocks tested. Shore scleroscope hardness was the only property that was similar for these rocks (85 to 105) and it will be shown in equation 14 that Shore hardness is related to crater width-crater depth.

To predict crater width for hard rocks with a Shore hardness between 85 and 105 and a density between 2.6 and 3.0, the following prediction equation was developed:

$$W = 0.017 + D\left(\frac{2.88}{SH} + \frac{7.88}{P}\right), \qquad (14)$$

where W = predicted crater width, inches,

D = crater depth, inches,

SH = Shore scleroscope hardness, scleroscope units,

and P = rock density, gram per cubic centimeter.

Equation 14 has a multiple correlation coefficient of 0.967 and a standard error estimate of 0.069. This equation was developed with the stepwise multiple linear regression analysis described earlier. Shore hardness and rock density were found significant at an F-level of 99.5 percent, and all other properties were rejected. The accuracy of this equation is demonstrated in figure 14.

Although equation 14 is designed to predict crater width for hard rocks, previous Bureau work in soft and medium rock made it possible to develop another predictor equation for both hard and soft rock. This equation would be used for rocks that had densities between 2.3 and 3.0 g/cm^3 and compressive strengths between 9,000 and 67,000 psi:

$$W = 0.025 + D\left(\frac{1.85\times10^4}{\sigma_c} + \frac{1.5\times10^1}{P}\right), \qquad (15)$$

where σ_c = unaxial compressive strength, pounds per square inch.

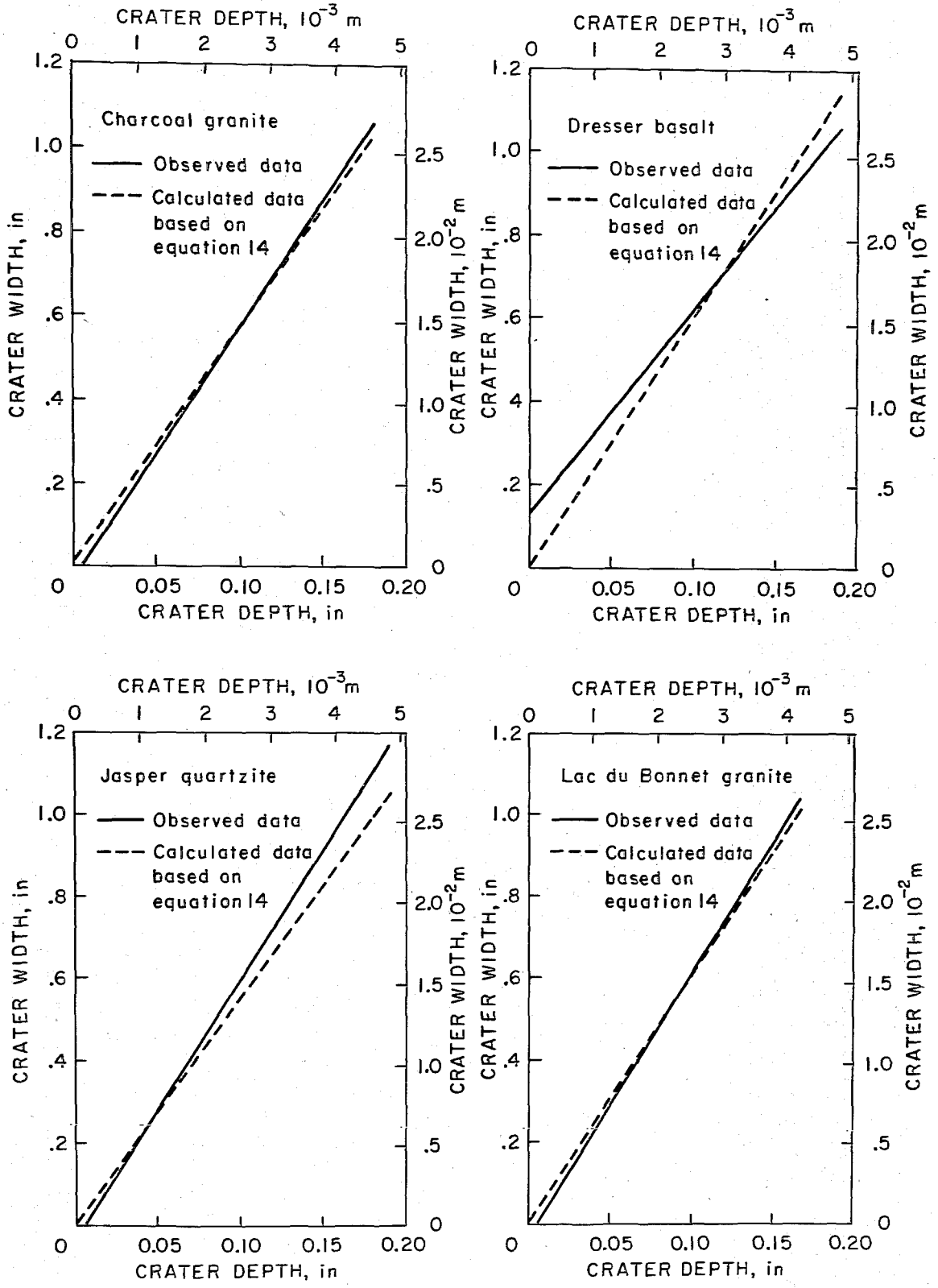

FIGURE 14. - Actual crater width versus predicted crater width (from equation 14) for hard rocks.

Equation 15 had a multiple correlation coefficient of 0.964 and a standard error of estimate of 0.092 in. This equation can be used for rocks with densities between 2.3 and 3.0 g/cm^3 and compressive strengths between 9,000 and 67,000 psi. The accuracy of this equation is shown in figures 15-16. Note that the calculated width is within 5 percent of the observed value for all the rocks.

Equations 14-15 are designed to estimate the crater width for a disk cutter with a 90° cutting edge only. Previous work with 60° cutting edges showed that it is possible to estimate crater width for a 60° cutter using the following relationship for identical normal cutter forces:

$$W_{60} = 1.32\ W_{90} \qquad (16)$$

A study of crater width has practical importance because it can be shown that the crater width of an independent crater is related to the optimum spacing of adjacent disk cutters in the laboratory. Optimum spacing is defined as the distance between two adjacent cutters where the maximum volume of material is removed or where specific energy is a minimum.

Bureau researchers have recently completed laboratory studies of the spacing of adjacent disk cutters (10). These researchers have determined the critical and optimum spacing of disk cutters in four rocks. Critical spacing is defined as the spacing at which interaction between adjacent craters first begins.

Although the determination of cutter spacing is a complex problem as fully described in the preceding reference, it appears possible to predict optimum disk cutter spacing from single crater studies. A comparison of single crater width with optimum cutter spacing for the four rocks tested in each of these studies was encouraging and is shown in table 6.

TABLE 6. - A comparison of single crater width and optimum cutter spacing

Rock type	Optimum spacing, in (at 7,000 lb normal force)	Single crater width, in (at 7,000 lb normal force)	Percent difference
Tennessee marble.....	0.646	0.588	-9.0
Valders white rock.....	.754	.738	-2.1
Charcoal granite.....	.459	.490	+6.3
Jasper quartzite.....	.387	.377	-2.6

Thus, the width of a single crater will serve as a good first approximation of the optimum spacing of adjacent cutters in the laboratory. Note, however, that the optimum cutter spacing should whenever possible be determined by experimentation since optimum spacing varies with normal cutter force and cutter diameter. The apparent relationship between single crater width and optimum cutter spacing is valid only for our laboratory work and cannot be used for boring machines in actual use.

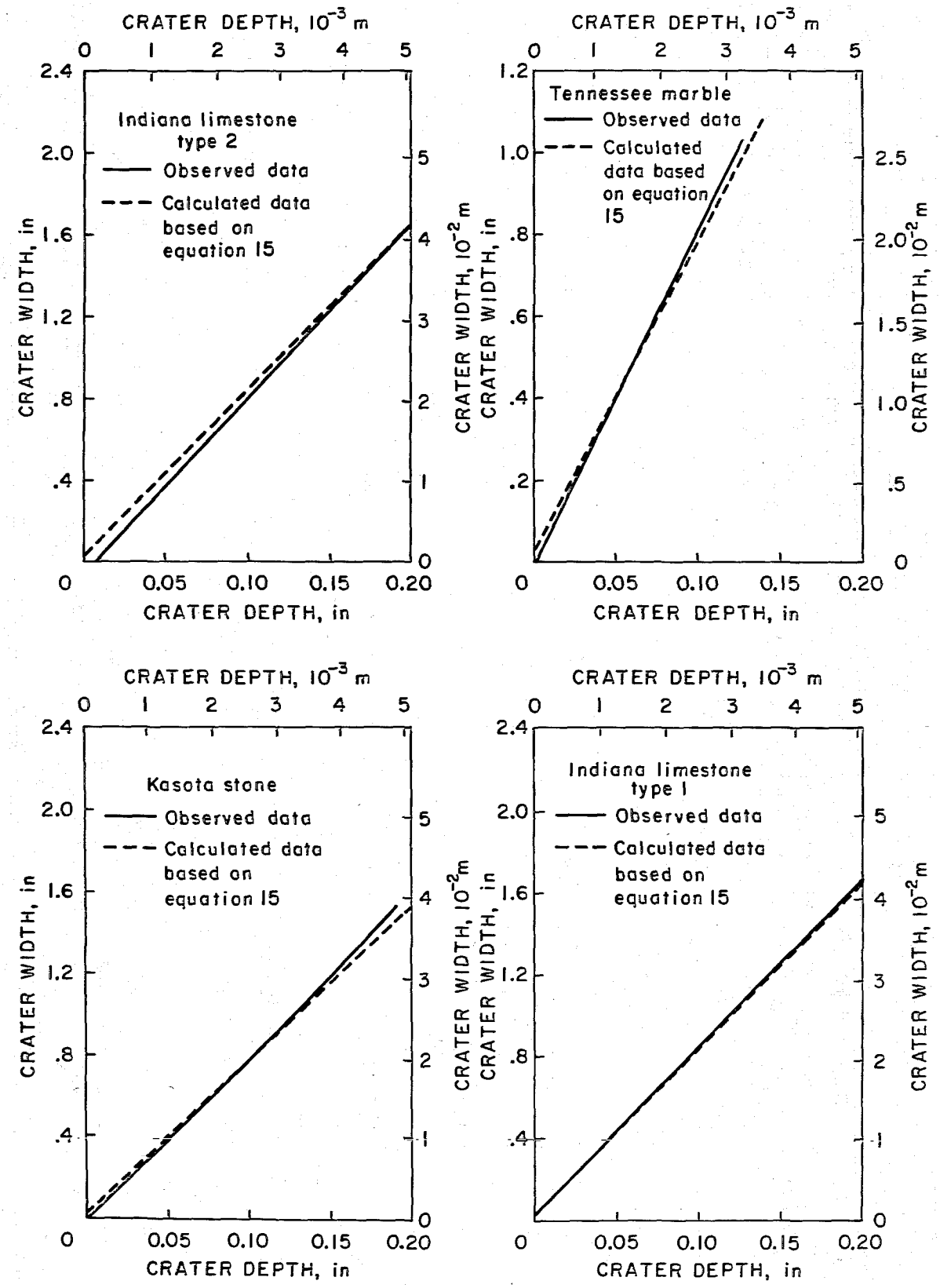

FIGURE 15. - Actual crater width versus predicted crater width (from equation 15) for soft and medium rocks.

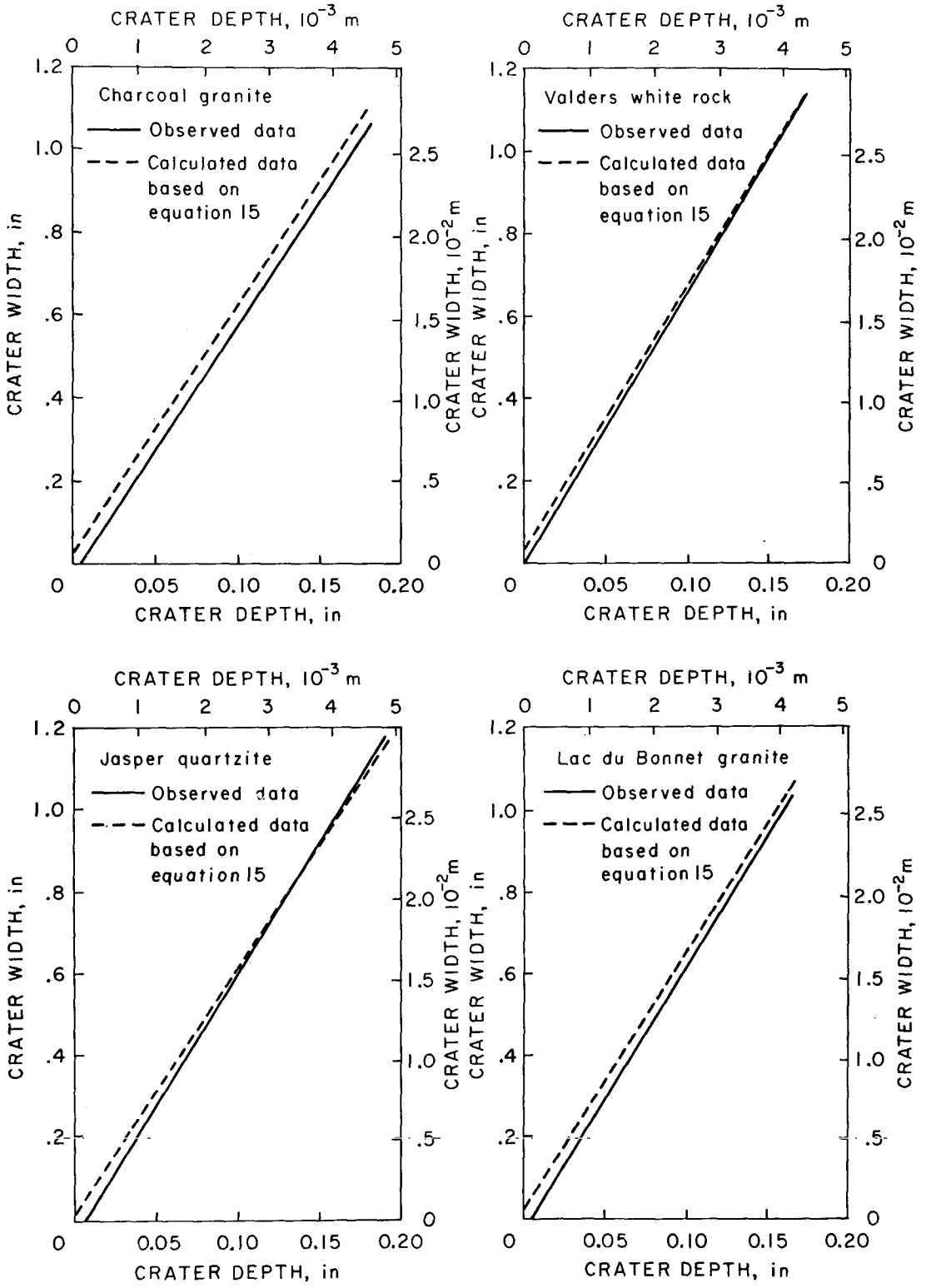

FIGURE 16. - Actural crater width versus predicted crater width (from equation 15) for medium and hard rocks.

Before concluding this section, it should be realized that although the four rocks tested had similar width-depth relationships, this does not mean that cutters with the same load will have the same crater depth or width. To determine how crater width is related to normal cutter force, the crater depth-normal force equations can be substituted in the equations in table 5 to yield the data given in table 7.

TABEL 7. - Crater width as a function of normal cutter force

Rock type	Crater width, in, as a function of normal cutter force, lb
Lac DuBonnet granite.....	$W = -0.03 + 1.60 \times 10^{-5} F_n^{1.16}$
Charcoal granite.....	$W = 0.02 + 2.01 \times 10^{-5} F_n^{1.14}$
Dresser basalt.....	$W = 0.13 + 2.35 \times 10^{-7} F_n^{1.59}$
Jasper quartzite.....	$W = -0.04 + 6.89 \times 10^{-6} F_n^{1.23}$

Because the rocks tested had very similar values of Shore scleroscope hardness, the crater width for these four rocks will be substantially the same at the same level of cutter load. For example, when evaluated at 14,000 lb normal force, the crater widths for these rocks (in order from top to bottom) are 0.967, 1.04, 1.04, and 0.85 in.

Crater Volume per Unit Length as a Function of Normal Cutter Force

Crater volume per unit length was chosen as a measure of crater size instead of simply volume since it was then possible to compare craters of different lengths. The volumes of the craters were calculated by dividing the weight of the chips formed during crater formation by the density of the rock. This volume was then divided by the crater length to yield volume per unit length, with units of cubic inches per foot (in^3/ft) or cubic centimeters per meter (cm^3/m).

Figure 17 shows crater volume per unit length as a function of normal cutter force for all four rocks tested. The equations of these curves are given in table 8. In all cases, the realtionship between crater volume per unit and normal cutter force was of this form:

$$V/L = KF_n^x \qquad (17)$$

where V/L = crater volume per unit length, cubic inches per foot,

K = a constant, cubic inches per foot pound^x,

F_n = normal cutter force, pounds,

and x = an exponent (see the following).

TABLE 8. - Crater volume per unit length as a function of normal force[1]

Rock type	Crater volume per unit length, in^3/ft, as a function of normal force, lb	S_e[2]
Lac du Bonnet granite.....	$V/L = 2.98 \times 10^{-10} F_n^{2.27}$	0.033
Charcoal granite.....	$V/L = 3.16 \times 10^{-9} F_n^{2.04}$	.048
Dresser basalt.....	$V/L = 4.95 \times 10^{-13} F_n^{2.96}$	.056
Jasper quartzite.....	$V/L = 8.06 \times 10^{-12} F_n^{2.61}$	.031

[1]The computer determined equations in the table are accurate to two significant figures.
[2]Standard error of estimate.

An analysis of figure 17 and table 8 shows that crater volume per unit length varied as the normal cutter force raised to a power between 2.0 and 2.9 for all rocks tested. In practical terms, this indicates that the efficiency of fragmentation process increases with increasing cutter load, and within the limits of cutter design, cutters should be loaded as heavily as possible to achieve good fragmentation.

Note that because the volume of rock broken for a field-scale mechanical boring device is very dependent on cutter spacing, the absolute values of crater volume obtained with the equations in table 8 will not be directly

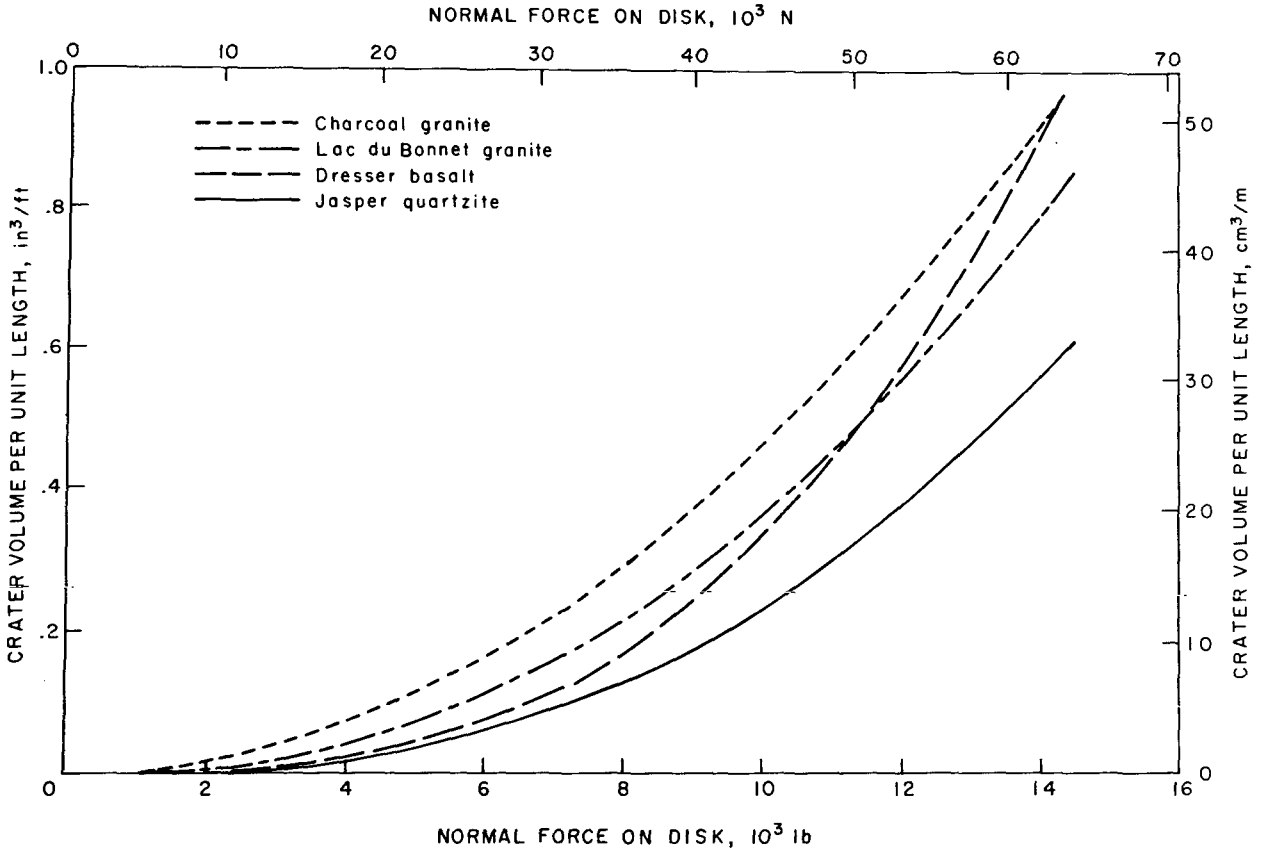

FIGURE 17. - Crater volume per unit length as a function of normal cutter force.

comparable. The values of crater volume obtained will still be useful, however, in comparing the realtive ease or difficulty of boring in different rock types and for comparing the relative efficiencies of different cutter types and configurations.

Energy-Volume Relationship

The energy required to form a crater with a disk cutter was defined as the sum of the vertical and horizontal work done by the disk. The vertical work was calculated by multiplying the average normal cutter force times the average crater depth, and the horizontal work was the average tangential cutter force times the length of the run. The vertical work was in all cases a small fraction of the horizontal work and can be eliminated without serious error.

Again, as noted previously, the tangential cutter force measured in these experiments is approximately 22 percent greater than the actual tangential cutter force that acts at the rock-cutter interface. Thus, the energy and specific energy data given in this report (which are computed from the tangential cutter force) will also be 22 percent larger than the actual values. Therefore, to obtain the absolute value of energy and specific energy, multiply the values given in this report by 0.78.

The crater volume as a function of energy for all the hard rocks tested is shown in figure 18. The best-fit equations of these curves are shown in table 9 and are of this form:

$$V = KE^x, \tag{18}$$

where V = crater volume, cubic inches,

E = energy, inch-pound,

K = a constant different for each rock, (cubic inches per inch-pound)^x,

and x = an exponent that varies between 1.2 and 1.4.

TABLE 9. - Crater volume as a function of input energy

Rock type	Crater volume, in^3, as a function of energy, in-lb	S_e[2]
Lac du Bonnet granite	$V = 4.11 \times 10^{-6} E^{1.26}$	0.073
Charcoal granite	$V = 4.21 \times 10^{-6} E^{1.22}$	.046
Dresser basalt	$V = 3.81 \times 10^{-7} E^{1.43}$	.120
Jasper quartzite	$V = 2.24 \times 10^{-6} E^{1.25}$	.049

[1]The computer determined equations in the table and equations 19 and 20 are accurate to two significant figures.

[2]Standard error of estimate.

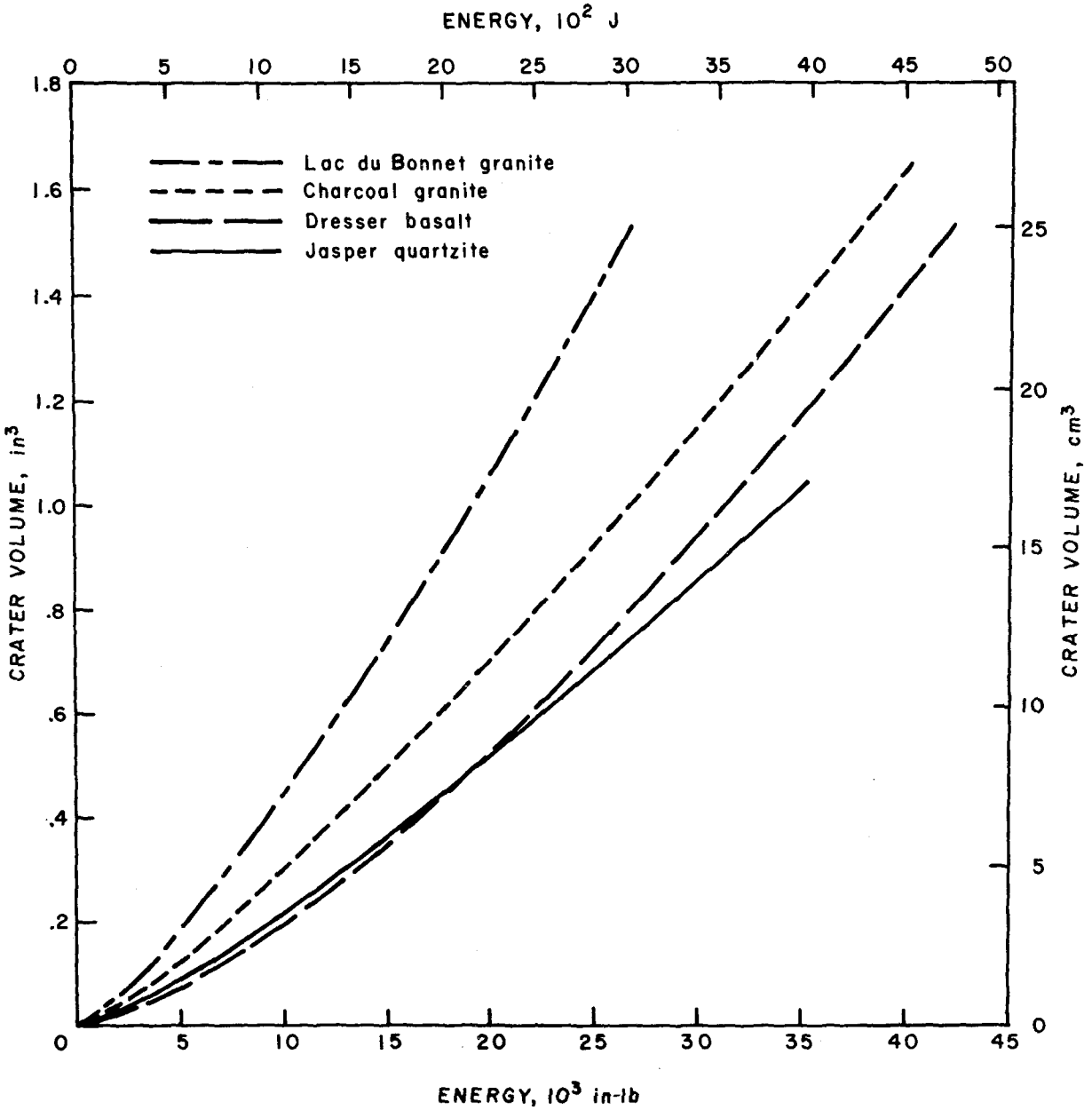

FIGURE 18. - Crater volume as a function of input energy.

From the equations and figures, it is observed that crater volume increases at an increasing rate with energy. This increase is slight, however, as the exponents are approximately 1.2 and may, for practical purposes, be estimated by a linear function (that is, x = 1.0). This is an important result since it shows that the volume of rock broken is directly related to the energy applied to the rock. For a given set of conditions, therefore, an increase in the energy applied to the rock will result in a proportional increase in the boring rate.

To predict crater volume for rocks other than those tested but with a Shore hardness between 85 and 105, a tensile strength between 1,100 and 2,000 psi, and a dynamic Young's modulus between 7×10^6 and 15×10^6 psi, the following prediction equation was developed:

$$V = -0.054 + E^{1.1}\left(\frac{1.48 \times 10^{-4}}{SH} + \frac{1.41 \times 10^{-2}}{\sigma_t} + \frac{3.74 \times 10^{1}}{YM_d}\right), \qquad (19)$$

where V = crater volume, cubic inches,

E = energy, inch-pound,

SH = Shore scleroscope hardness, scleroscope units,

σ_t = uniaxial tensile strength, pounds per square inch,

and YM_d = dynamic Young's modulus, pounds per square inch.

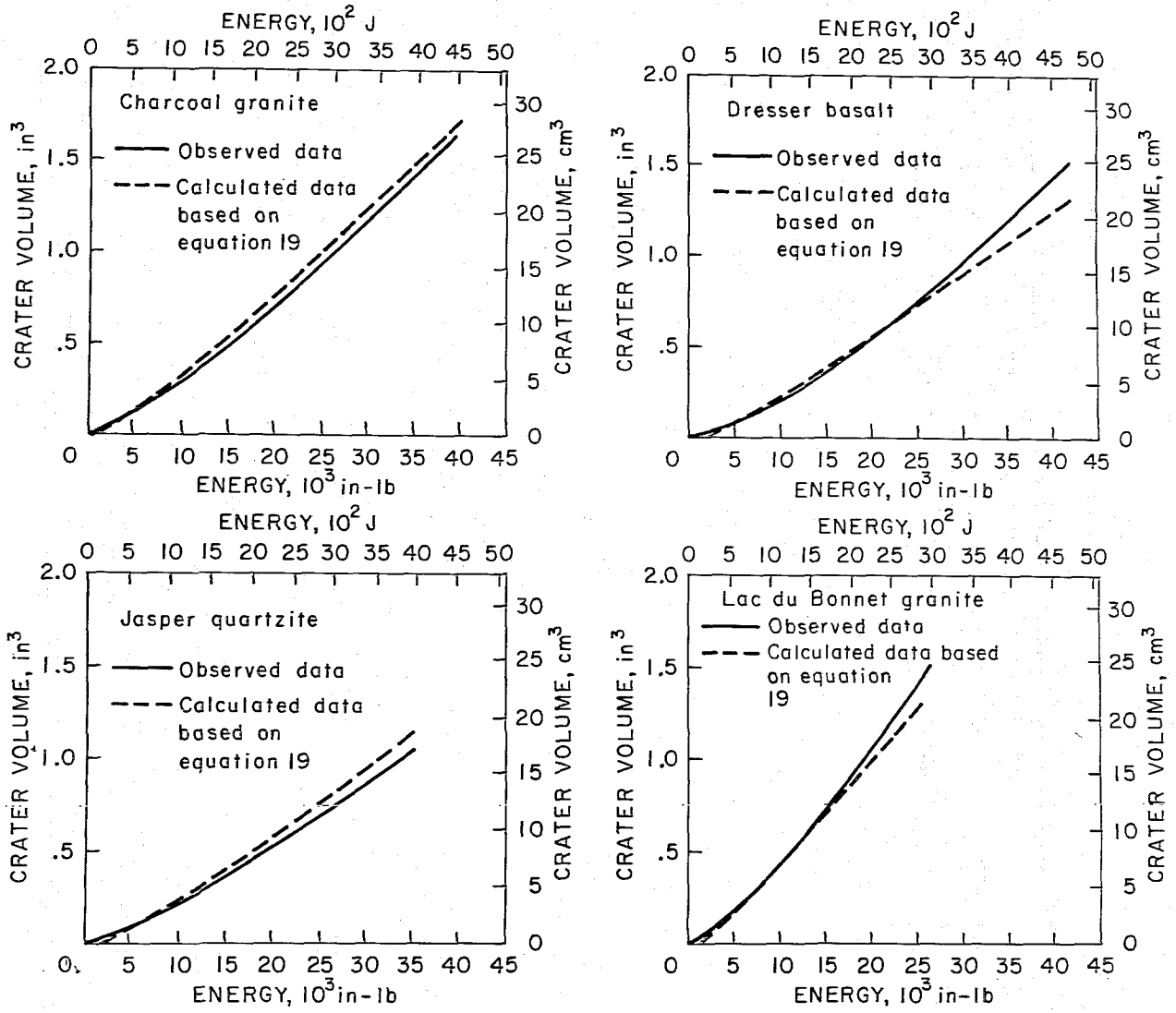

FIGURE 19. - Actual crater volume versus predicted crater volume (from equation 19) for hard rocks.

Equation 19 has a multiple correlation coefficient of 0.981 and a standard error of estimate of 0.087 in^3. The accuracy of this equation is demonstrated in figure 19.

One other predictor equation for crater volume was developed that combined both hard rock data and soft rock data. This equation can be used to predict crater volume for rocks that fall between the soft and the hard rocks studied in these experiments:

$$V = -0.090 + E\left(\frac{8.43 \times 10^{-1}}{\sigma} + \frac{8.48 \times 10^{-4}}{SH} + \frac{6.67 \times 10^{1}}{SM}\right). \qquad (20)$$

Equation 20 can be used for rocks with a Shore scleroscope hardness between 27 and 105, and with compressive strengths between 9,000 and 67,000 psi, and shear modulus (SM) between 2.1 and 6.14 $\times 10^6$ psi. The predictor equation had a multiple correlation coefficient of 0.983 and a standard error of estimate of 0.127 in^3. The accuracy of the equation is demonstrated in figures 20-21. In all but one of the rocks tested the predicted values is within 7 percent of the observed values.

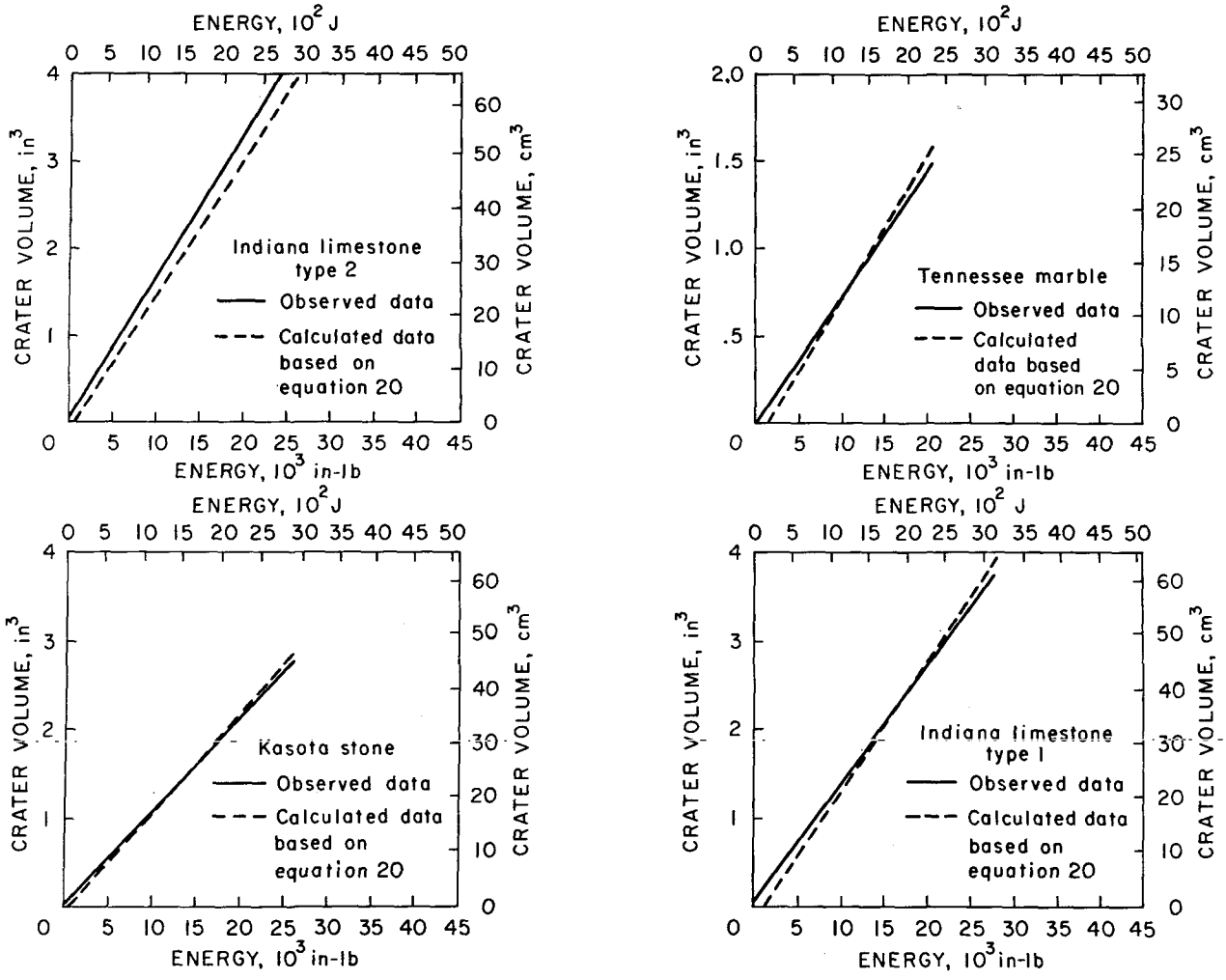

FIGURE 20. - Actual crater volume versus predicted crater volume (from equation 20) for soft and medium rocks.

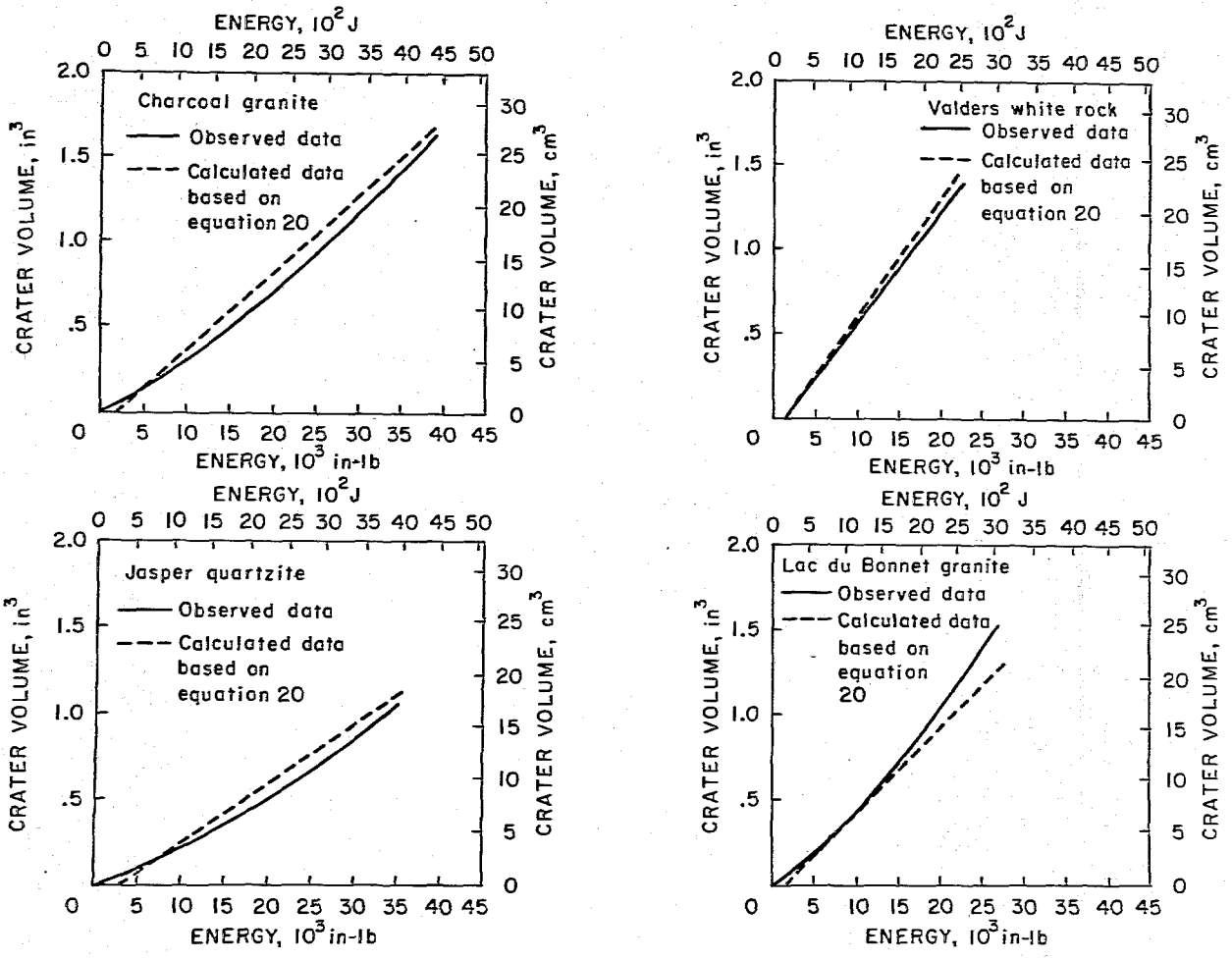

FIGURE 21. - Actual crater volume versus predicted crater volume (from equation 20) for medium and hard rocks.

Prediction equations 19-20 must be used with caution since the volume obtained in single-crater studies is quite different from that obtained with actual multicutter boring machines. In addition, the input energy cannot be varied at will but is itself a function of normal cutter force. However, equations 19-20 are useful in defining how crater volume is related to rock properties and input energy and can be used as a check on the boring rates and torque calculated from prediction equations 4-5, and 9-10. A more useful quantity that relates both volume and energy as a function of normal cutter force is specific energy, and this quantity is defined and discussed in the following section.

Specific Energy as a Function of Normal Cutter Force

Specific energy is a measure of the relative efficiency of the rock breakage process and is defined as the energy required to break out a unit volume of rock. This is written as follows:

$$E_s = \frac{\text{Input Energy (in-lb)}}{\text{Crater Volume (in}^3\text{)}} \qquad (21)$$

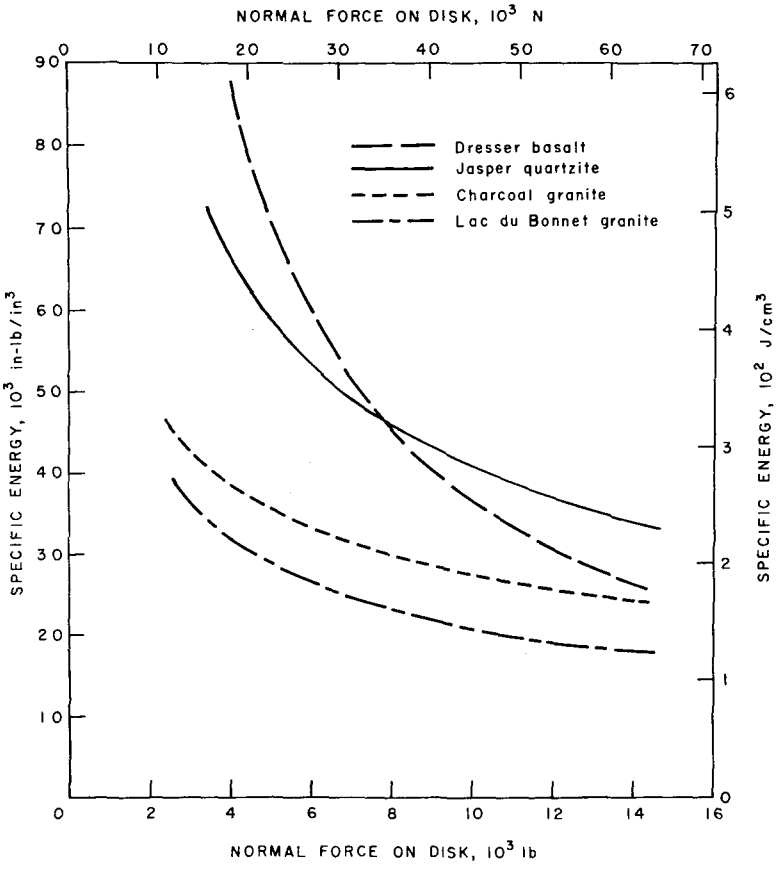

FIGURE 22. - Specific energy as a function of normal cutter force.

It was found that specific energy is not a constant but varies as a function of the normal cutter force. This is shown in figure 22 and the equations of these curves are shown in table 10. The equation that best describes the specific energy-normal force relationship is as follows:

$$E_s = KF_n^{-x}, \qquad (22)$$

where E_s = specific energy, inch-pound per cubic inch,

F_n = normal cutter force, pounds,

K = a constant different for each rock, inch-pound $^{(1 + x)}$ per cubic inch,

and x = an exponent.

TABLE 10. - Specific energy as a function of normal force[1]

Rock type	Specific energy, in-lb/in^3, as a function of normal force, lb	S_e[2]
Lac du Bonnet granite.....	$E_s = 1.58 \times 10^6 F_n^{-.47}$	2,880
Charcoal granite.....	$E_s = 8.02 \times 10^5 F_n^{-.37}$	1,880
Dresser basalt.....	$E_s = 2.74 \times 10^8 F_n^{-.97}$	8,380
Jasper quartzite.....	$E_s = 6.40 \times 10^6 F_n^{-.55}$	6,750

[1]The computer determined equations in the table are accurate to two significant figures.

[2]Standard error of estimate.

Figure 22 shows that specific energy decreases as normal force is increased, rapidly at first and then approaching a steady-state value. Previous work in soft rock shows that specific energy also became a constant but more quickly than for the hard rocks. It is apparent from this that the normal force acting on a cutter should be large enough so that the specific energy is on the flat portion of the curve. Fortunately this requires only a small portion of the load normally applied to cutters in actual practice. Many researchers, including the Bureau, have used the ratio of specific energy

and rock compressive strength as an indication of the efficiency of the rock fragmentation process. F. Gaye calls the inverse of this ratio the rock number (2). The smaller the specific energy the larger the rock number and the more efficient the fragmentation process. Compressive strength is used as the basis of comparison because it is the most widely used and most readily available of all the rock physical properties. Since specific energy varies with normal cutter force, it is necessary to choose a specific point on the curve (fig. 22) where specific energy begins to level off. This point should also represent a reasonable field value for a full-scale boring machine. Specific energy at a normal force of 14,000 lb and the ratio of specific energy and uniaxial compressive strength are given in table 11.

TABLE 11. - The ratio of specific energy and rock compressive strength for laboratory disk cutters

Rock type	Compressive strength, psi	Specific energy (calculated at F_n = 14,000 lb) in-lb/in^3	Ratio of specific energy and compressive strength
Lac du Bonnet granite.....	38,300	18,000	0.47
Charcoal granite.....	39,110	27,000	.69
Dresser basalt.....	63,610	30,000	.47
Jasper quartzite.....	67,470	34,000	.50

The specific energies obtained for these single-crater studies will not be applicable to those obtained for real mechanical boring machines since there was no breaking of material between adjacent craters. These values are therefore the absolutely worst case conditions for a real boring machine.

Table 12 illustrates the actual range of the specific energy-compressive strength ratio obtained for full-scale mechanical boring machines.

TABLE 12. - The ratio of specific energy and rock compressive strength for tunnel boring machines (3)

Project	Average rock hardness (compressive strength), psi	Specific energy, in-lb/in^3	Ratio of specific energy and rock strength
Port Huron, Mich.....	12,000	2,250	0.19
Lawrence Ave., Chicago, Ill.....	30,500	6,620	.22
Cookhouse, South Africa.....	40,000	5,950	.15

An increase in normal cutter force not only reduces specific energy but also changes the character of the rock broken from the craters. At higher cutter loads the cutter produces larger rock chips with proportionately less pulverized material formed. A sieve analysis performed on soft rocks in another study, which is also applicable to the hard rocks in this study, shows that larger rock fragments and fewer fines are produced both at higher cutter loads and with sharper cutting edges. These conditions are shown in figures 23-24. Typical rock fragments produced by a disk cutter are shown in figure 25.

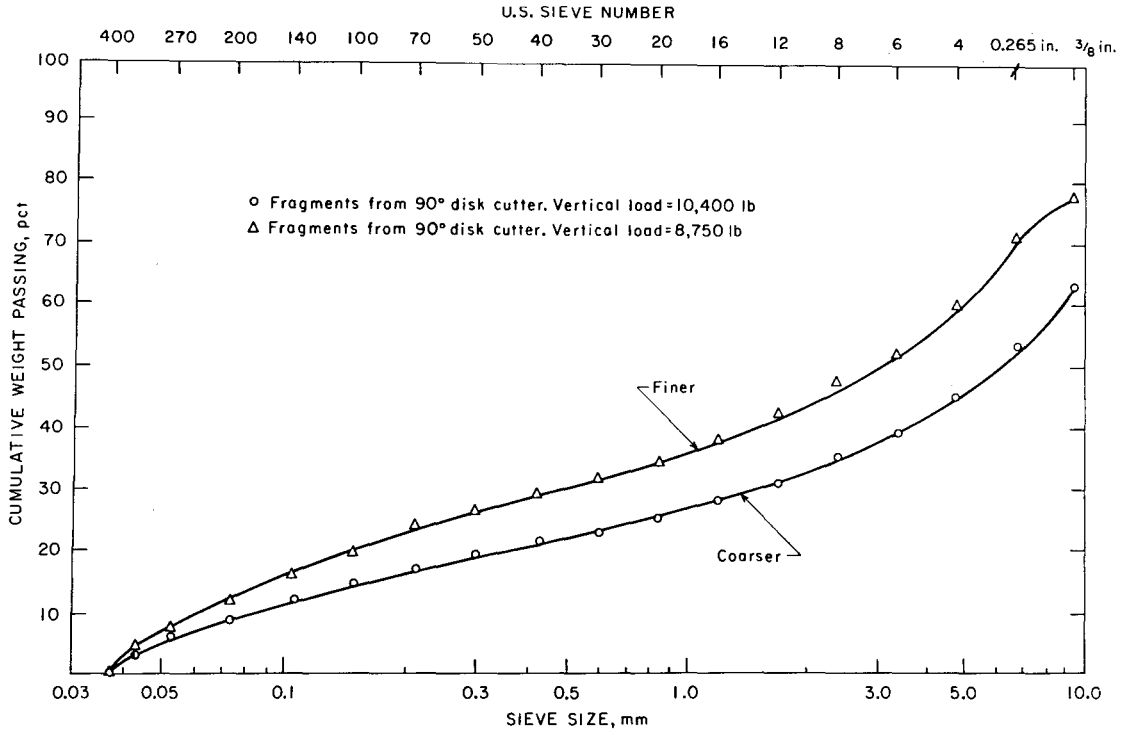

FIGURE 23. - Cumulative logarithmic diagram of a screen analysis of rock fragments produced by a 90° disk cutter at different normal loads.

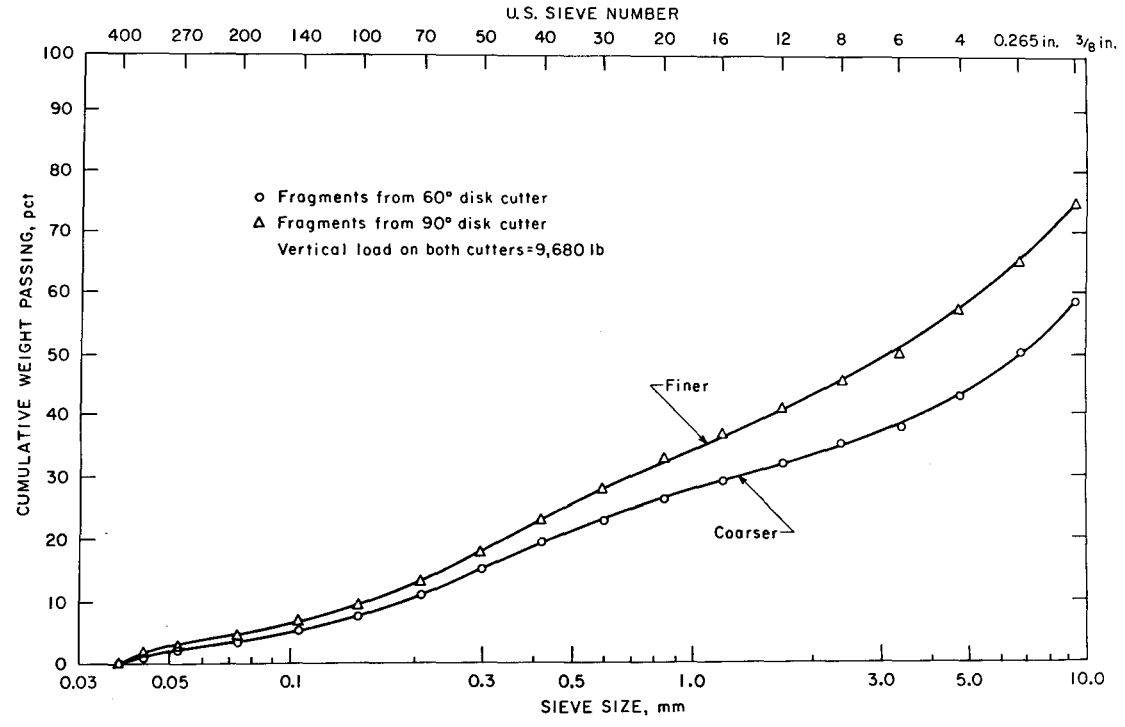

FIGURE 24. - Cumulative logarithmic diagram of a screen analysis of rock fragments produced by a 60° and 90° disk cutter at the same normal load.

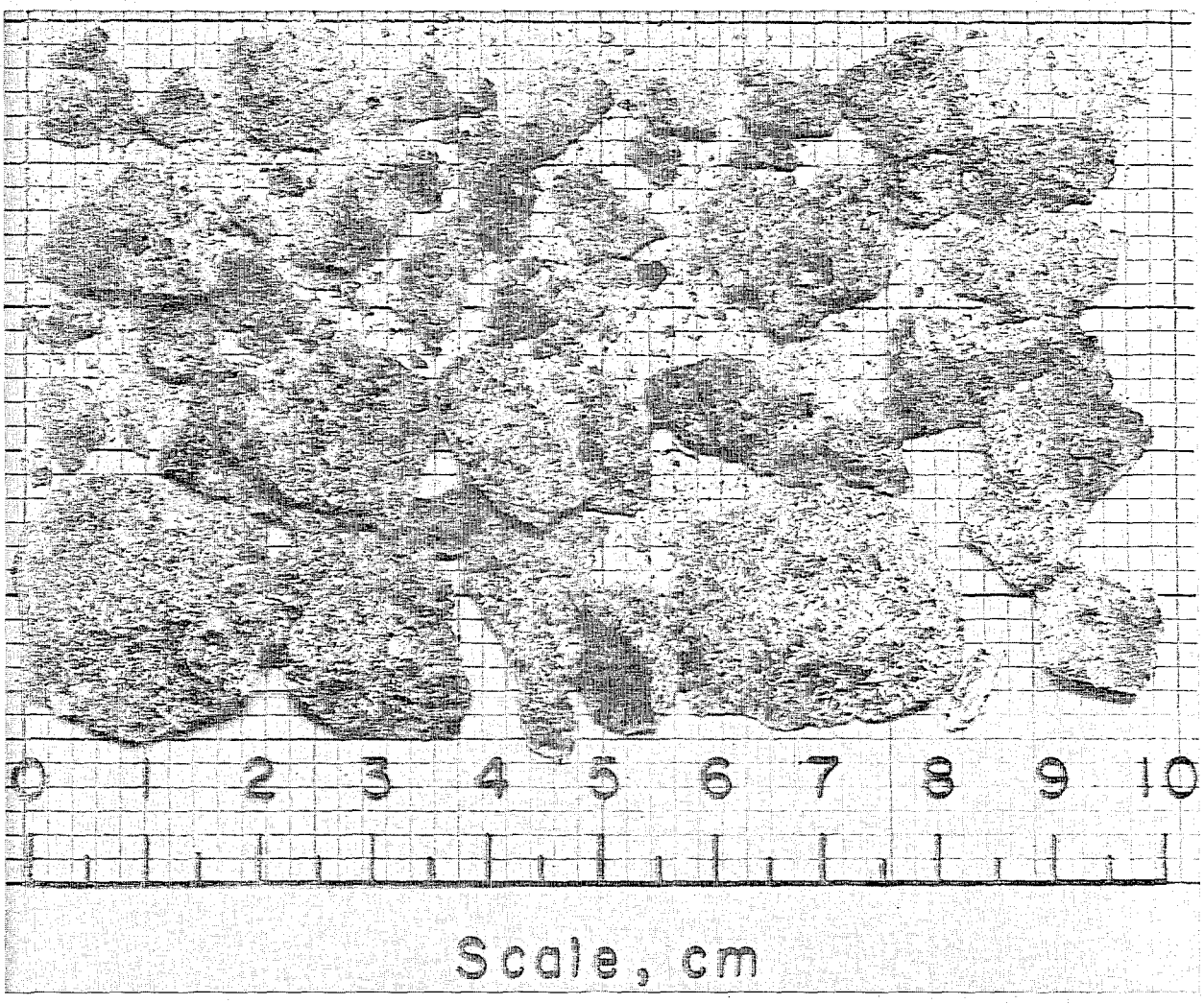

FIGURE 25. - Typical rock fragments produced by a disk cutter.

The usefulness of laboratory values of specific energy just discussed is limited to comparing the relative ease or difficulty of boring different rocks. They cannot be used as absolute values since the laboratory experiments were not designed to duplicate field boring conditions.

DISCUSSION OF RESULTS

Since the disk cutter experiments reported herein were designed primarily to define the fundamental relationships governing disk-cutter performance, they were performed under a narrow range of experimental conditions including linear motion, single-crater studies, absence of indexing effects, smooth rock surfaces, and the constant cutter geometry. Hence, the constants of proportionality found in the equations will not be appropriate under field boring conditions. However, some of the more important experimental results that may be of immediate value to those engaged in the design or use of mechanical excavation equipment utilizing disk cutters are now discussed.

Boring Rate

During these and previous experiments with disk cutters, the following factors were found to be directly related to the depth of penetration of a disk cutter and hence to the boring rate of a mechanical boring machine.

1. The depth of penetration of a disk cutter is a function of the normal force acting on the cutter raised to a power typically between 1.0 and 1.2. Any increase in normal cutter force will result in a proportional or somewhat greater than proportional increase in the depth of penetration. Since the effect of reducing cutter diameter is to increase the local stress under the cutter (at the same normal force), small-diameter cutters will penetrate deeper than large-diameter cutters. The use of smaller diameter disk cutters on a boring machine would reduce the total thrust requirement or alternatively would increase the boring rate at the same level of thrust.

2. Disk cutters with sharper cutting edges will penetrate rock faster and with less energy consumption than cutters with blunter cutting edges. For example, it was experimentally determined that a 60° cutting edge penetrated an average of 1.67 times deeper than a 90° cutting edge at the same level of normal force. Therefore boring machine cutters should have the sharpest cutting edge possible consistent with good wear resistance.

3. In the laboratory, it was found that the depth of penetration of a disk cutter could be accurately determined from a prediction equation involving normal cutter force and the following rock properties: Shore scleroscope hardness, static Young's modulus, and rock density (equations 4-5). Although these predictor equations have not yet been proven for actual field use, it is suggested that the following method of calculation could be used to determine a preliminary estimate of potential boring rate. To illustrate, if a boring machine achieved an advance rate of 10 fph in a rock that had a calculated crater depth of 0.2 in (from equation 4 or 5), then it would be expected that the same machine could bore at 5 fph in a rock with a calculated crater depth of 0.1 in, at the same load (p. 15). Experiments at the Bureau's Twin Cities Mining Research Center are currently underway to determine if the aforementioned hypothesis is correct.

Cutter Spacing

The average width of single craters formed with a disk cutter has been found to be highly related to the optimum indexing distance between adjacent disk cutters in the laboratory. Optimum indexing distance is the distance between adjacent cutters at which point a maximum volume of rock is broken or where specific energy is at a minimum. Although this technique of determining optimum cutter spacing has only been investigated in the laboratory, it is hoped that when a suitable multiplication factor is found, it will serve as a first approximation for full-scale boring machines. The use of the optimum indexing distance is illustrated in item 3 of this section.

To determine the optimum cutter spacing of adjacent cutters, the width of a single crater is determined at the same conditions that will be encountered

in the field. This is necessary since crater width is highly related to the following factors:

1. Crater width is a linear function of crater depth. Thus doubling the normal cutter force will double the crater depth and hence the crater width. Crater width must be evaluated at the same level of normal force that is expected in the field.

2. Crater width is also related to the cutting edge of the disk cutter. For example, it has been experimentally determined that a 60° cutting edge will produce a crater approximately 1.32 times wider than a 90° cutting edge with the same normal cutting force. In general, the sharper the cutting edge, the wider the crater that will be produced.

3. Crater width was also found to be highly related to the following rock physical properties: Shore scleroscope hardness, rock density, and rock compressive strength (equations 14-15). Again, although the technique of using single crater width to determine optimum cutter spacing has not been verified in field use, it is suggested that the following method of calculation could be used as a preliminary estimate if no other data were available. If a boring machine with an optimum cutter spacing of 3 inches works well in a rock with a calculated crater width of 1.0 in (equations 14-15), then a cutter spacing of 2.0 in would be expected to be optimum in a rock with a calculated crater width of 0.66 in. If laboratory conditions could exactly duplicate field conditions, then the laboratory value of single crater width would be exactly equal to the optimum cutter spacing on a full-size machine.

Boring Machine Torque

The torque required to rotate the cutterhead of a mechanical boring machine is dependent upon the distance that the individual cutters are positioned from the center of the cutterhead and the tangential force acting on each cutter. Although the total torque arm is easily calculated from the cutterhead drawings, the value of the tangential cutter force can only be estimated from previous experience. To aid in the estimate of this highly important quantity, the following experimental results are presented:

1. The tangential force acting on a disk cutter is a function of the normal cutter force raised to a power between 1.5 and 2.0. This exponent is lower for the softer rocks and higher for the harder rocks. Thus, for example, doubling the normal cutting force will result in threefold increase in tangential cutting force in soft rocks, and a fourfold increase in tangential cutting force in hard rocks. For the conditions defined in this study, the maximum tangential cutter force varied between 0.07 and 0.14 times the normal cutting force, depending on rock type.

2. The tangential cutting force was found to be a function of the normal cutting force and the following rock properties: Shore scleroscope hardness and rock density. A prediction equation using these parameters was developed for hard rocks and for combined hard and soft rocks (equations 9-10). Note that although tangential cutting force increases faster with increasing

normal force for hard rocks (see item 1 above), the absolute magnitude of tangential force will be larger for the softer rocks; that is, rocks with low values of Shore hardness and rock density. These equations can be used to predict cutterhead torque given the torque on a completed job and the calculated tangential cutting force for both jobs. The procedure would be to compare the ratio of the predicted tangential cutter forces with the ratio of the actual cutterhead torque and the unknown cutterhead torque. The unknown cutterhead torque can be solved directly from the ratio but note that this procedure is valid only if the two cutterheads in question are identical.

3. Since it has been shown that crater volume is approximately a linear function of input energy (equation 18), it follows that increasing the input energy to the rock will increase the volume of rock removed and hence the boring rate. The input energy to the rock is a product of the cutterhead torque and cutterhead rpm, and cutterhead torque in turn is a product of the torque arm and the tangential cutter force. Thus, increasing the cutterhead torque will increase the input energy and rate of volume removed. Therefore, to make disk cutters capable of applying more energy to the rock face, it is necessary to increase the ratio of the tangential and normal cutting forces (that is, coefficient of friction) acting on these cutters. The only known ways of doing this at the present are to increase the normal force on cutters (or alternatively decrease the cutter diamter) or to use cutters with sharper cutting edges. It is suggested that other means of increasing the coefficient of friction be investigated.

Energy Considerations

The energy required to fragment a unit volume of rock is a useful indication of boring efficiency. Lower specific energy signifies a more efficient excavation process and is a goal to which machine designers must strive. The three major conclusions determined in a study were:

1. Specific energy is not a fixed quantity but varies inversely with normal cutter force. At low values of cutter thrust, the specific energy is high, and as thrust is increased, the specific energy decreases rapidly and then approaches a steady-state value. The value of cutter thrust at which point specific energy approaches a steady value was for the hard rocks approximately 8,000 lb and for the soft rocks approximately 4,000 lb. The practical implication of this is that cutters should be loaded with enough force to be in the efficient excavation region.

2. Disk cutters with sharper cutting edges are more efficient and have lower specific energies than cutters with blunter edges. It was determined experimentally that a cutter with a 60° cutting edge broke out approximately 40 percent more rock than did a 90° edge for the same amount of input energy. Manufacturers should use the sharpest cutting edges possible consistent with good wear and breakage characteristics.

3. The ratio of specific energy and rock compressive strength was relatively constant for all the rocks tested in the laboratory. It ranged from 0.47 to 0.69 with an overall average of 0.53 for the hard rocks and 0.60

0.80 for the soft rocks. If the ratio of specific energy and compressive strength can be shown to be a constant for field boring also, then the energy required by a boring machine to break out a given volume of rock can be determined. Once the energy is known, the size of the cutterhead drive motors can be determined independently of the torque calculations given previously. Note that the ratio of specific energy and compressive strength for full-scale boring machines ranged from 0.15 to 0.22, which is two to six times smaller than the authors' laboratory values. It must be realized that although a constant E_s/σ_c ratio indicates that for a given amount of input energy a given volume of rock is broken, it does not guarantee that a given energy can be put into the rock. For example, in a hard rock, the maximum normal thrust on the cutters may produce a tangential force that is insufficient to achieve the designed input energy and hence the desired boring rate.

CONCLUSIONS

During this study separate results were obtained for a series of hard rocks and for a combination of soft, medium, and hard rocks. It is suggested that the results for the combination soft, medium, and hard rocks be used unless the rock in question clearly falls into the hard rock group. The use of the following relationships and prediction equations are illustrated in the "Discussion of Results" section.

1. The following important relationships were defined in this study for a combination of soft, medium, and hard rocks: (1) Crater depth is a linear function of normal cutting force, (2) tangential cutting force is a function of the normal cutting force raised to the 1.9 power, (3) crater width is a linear function of crater depth, (4) crater volume is a linear function of input energy, and (5) specific energy is a function of normal cutting force raised to the -0.5 power.

2. Standard rock physical properties used singly or in combination have been effective in predicting disk cutter performance in a variety of rock types. Equations were developed to predict crater depth, crater width, crater volume, and tangential cutter force as a function of the following rock properties: Shore scleroscope hardness, density, static Young's modulus, compressive strength, tensile strength, and dynamic Young's modulus. These prediction equations can be used to estimate the boring rate, the cutter spacing, and the torque and energy requirements of a full-scale boring machine as illustrated in the "Discussion of Results" section.

3. Penetration rate and specific energy were found to be highly dependent upon normal cutter force. To obtain high penetration rates and low specific energy, disk cutters should be loaded as heavily as possible consistent with reasonable cutter and bearing wear. An alternative to increasing the cutter load is to reduce the diameter of the disk cutter.

4. Penetration rate and specific energy were also found to be highly dependent upon the sharpenss of the cutting edge. The sharpest cutting edge consistent with good wear characteristics should be used to maximize penetration rate and decrease specific energy.

5. To increase penetration rate, tangential cutting force should be maximized because this parameter accounts for the bulk of the energy consumed during rock cutting. Presently this can be done only by increasing the normal force on the cutter and by using a sharper cutting angle. It is suggested that other means to increase tangential cutter force be investigated.

REFERENCES

1. Environmental Protection Agency. Proceedings From Deep Tunnels in Hard Rock - A Solution to Combined Sewer Overflow and Flooding Problems. An Engineering Institute by the University of Wisconsin - Milwaukee, Wis., Nov. 9-10, 1970, 221 pp.

2. Gaye, F. Efficient Excavation With Particular Reference to Cutting Head Design of the Hard Rock Tunneling Machines. Tunnels and Tunneling, pt. 1, January-February, 1972, pp. 39-48; pt. 2, March-April, 1972, pp. 135-142.

3. Hustrulid, W. A. A. Theoretical and Experimental Study of Tunnel Boring by Machine With an Emphasis on Boreability Prediction and Machine Design. Colo. School Mines, Golden, Colo., Interim Final Report on Bureau of Mines Contract H0210043, Feb. 19, 1972, 260 pp; available from National Technical Information Service, Springfield, Va., AD 762 427.

4. Organization for Economic Cooperation and Development. Report on Tunneling Demand 1960-1980. Advisory Conf. on Tunneling, Washington, D.C., June 22-26, 1970, 160 pp.

5. Miller, I., and J. E. Freund. Probability and Statistics for Engineers. Prentice-Hall, Inc., Englewood Cliffs, N.J., pp. 226-249.

6. Mood, A. M., and F. A. Graybill. Introduction to the Theory of Statistic Statistics. McGraw-Hill Book Co., Inc., New York, 2d ed., 1963, pp. 328-355.

7. Morrell, R. J., W. E. Bruce, and D. A. Larson. Tunnel Boring Technology--Disk Cutter Experiments in Sedimentary and Metamorphic Rocks. BuMines RI 7410, July 1970, 32 pp.

8. National Academy of Sciences. Rapid Excavation: Significance, Needs, Opportunities. Washington, D.C., 1968, p. 48.

9. Rad, P. F., and F. J. McGarry. Thermally Assisted Cutting of Granite. Proc. 12th Rock Mech. Symp., Univ. of Mo., Rolla, Mo., Nov. 16-18, 1970, The American Institute of Mining, Metallurgical, and Petroleum Engineers, Inc., New York, 1971, pp. 721-757.

10. Rad, P. F., and R. C. Olson. Tunnel Machine Research--Interaction Between Disk-Cutter Grooves in Rock. BuMines RI 7881, 1974, 21 pp.

11. Takaoka, S., H. Hayamizu, and S. Misawa. Studies on the Cutting of Rock by Rotary Cutters - Part I: Rock Cutting by Disc Cutters. J. Min. Met. Inst. of Japan, v. 84, No. 960, 1968-69, pp. 427-432. (Translated from Japanese by Y. Kojima and W. Hustrulid, Colo. School Mines, Golden, Colo.)

APPENDIX

TABLE A-1. - Description of symbols

Symbols	Description	Appears in	
		Equation	Table
$B_{(\ )}$	Instantaneous boring rate (subscripted for different rock types).	7	-
$D_{(\ )}$	Crater depth, in (subscripted for cutter edge angle and different rock types).	3-7 and	2 and 5
E	Energy, in-lb	18-20	9
E_s	Specific energy, in-lb/in^3	22	12
F_n	Normal cutter force, lb	3-5, 8-12, 17 and 22	2, 4, 7 and 8
$F_{t_{(\ )}}$	Tangential cutter force, lb (subscripted for cutter edge angle).	8-11	4
R_i	Distance from cutter head center to cutter, ft	12	-
T	Cutter head torque, ft-lb	12	-
V	Crater volume, in^3	18-20	9
V/L	Crater volume per unit length, in^3/ft	17	8
$W_{(\ )}$	Crater width, in (subscripted for cutter edge angle).	13-16	5 and 7
P	Apparent density, g/cm^3	5, 10, 14 and 15	-
SH	Shore hardness, scleroscope units	4, 5, 9, 10, 14, 19 and 20	-
SM	Shear modulus, psi	20	-
$YM_{(\ )}$	Young's modulus (subscripted d and s for dynamic and static, respectively).	4, 5, and 19	-
σ_c	Compressive strength, psi	15 and 20	-
σ_t	Tensile strength, psi	19	-

TABLE A-2. - Data from linear cutter tests

Test	Average forces, lb		Crater measurements			Average forces, lb		Crater measurements		
	Normal	Tangential	Width, in	Depth, in	Volume, in^3	Normal	Tangential	Width, in	Depth, in	Volume in^3
	Lac du Bonnet granite					Charcoal granite				
1	2,728	38	0.10	0.017	0.017	2,415	87	0.15	0.022	0.039
2	3,304	73	.14	.024	.048	3,969	222	.27	.037	.109
3	5,050	196	.27	.051	.124	4,890	318	.31	.057	.169
4	5,883	252	.35	.057	.222	6,481	515	.44	.073	.331
5	6,774	314	.40	.068	.252	6,963	577	.51	.079	.372
6	8,067	411	.48	.079	.368	7,892	738	.53	.092	.513
7	8,966	476	.54	.082	.437	9,040	846	.62	.110	.647
8	9,786	567	.67	.090	.560	7,981	788	.56	.096	.559
9	10,894	680	.77	.116	.821	11,033	1,328	.89	.146	1.107
10	11,791	831	.72	.126	.804	12,007	1,511	.99	.156	1.310
11	12,802	970	.77	.130	.115	13,101	1,649	.86	.157	1.185
12	14,227	1,071	.97	.145	.448	14,255	1,980	1.01	.175	1.671
13	10,574	678	.67	.109	.615	4,900	323	.38	.056	.178
14	4,583	161	.25	.052	.098	4,054	249	.26	.043	.125
15	4,435	156	.24	.050	.106	5,972	467	.43	.072	.290
16	4,192	119	.20	.042	.074	7,910	683	.46	.092	.422
17	6,232	259	.33	.062	.203	6,986	736	.47	.098	.543
18	7,009	371	.46	.077	.359	8,961	990	.63	.117	.650
19	7,960	459	.59	.082	.435	10,069	1,089	.71	.122	.877
20	9,100	546	.58	.098	.535	11,007	1,246	.79	.135	.925
21	11,120	749	.74	.115	.780	11,120	1,395	.82	.149	1.115
22	12,096	929	.75	.137	.951	12,162	1,527	.87	.156	1.201
23	12,848	968	.89	.136	.095	13,314	1,715	1.02	.165	1.511
24	13,614	1,071	.91	.150	.307	12,852	1,549	.83	.153	1.194
25	6,091	296	.38	.061	.248	14,170	1,842	1.01	.169	1.359
26	4,906	186	.29	.046	.142	6,948	603	.51	.081	.363
27	4,288	148	.25	.040	.104	3,934	224	.24	.042	.115
28	3,337	96	.17	.028	.060	5,074	369	.35	.054	.196
29	2,678	60	.12	.021	.043	6,089	512	.47	.067	.306
30	4,314	131	.24	.040	.090	9,132	950	.69	.110	.655
31	5,178	193	.29	.055	.150	10,107	1,104	.76	.119	.798
32	6,049	240	.35	.060	.216	12,134	1,419	.87	.144	1.212
33	7,060	349	.42	.076	.303	12,076	1,448	.88	.140	1.117
34	6,881	403	.51	.083	.405	14,051	1,868	.99	.177	1.578
35	8,960	519	.53	.094	.524	14,085	1,827	1.09	.171	1.534
36	10,102	697	.62	.114	.688	13,059	1,512	.88	.147	1.104
37	10,813	686	.73	.118	.719	11,075	1,223	.90	.134	.973
38	11,850	805	.82	.124	.895	8,923	865	.72	.104	.604
39	13,395	962	.91	.139	.270	7,973	727	.57	.092	.512
40	14,185	1,240	.98	.158	.416	4,935	326	.36	.056	.182
41	13,761	1,122	.87	.143	.152	3,256	141	.21	.033	.078
42	12,890	912	.96	.140	.280	-	-	-	-	-
43	4,990	186	.26	.048	.152	-	-	-	-	-

TABLE A-2. - Data from linear cutter tests--Continued

Test	Average forces, lb		Crater measurements			Average forces, lb		Crater measurements		
	Normal	Tangential	Width, in	Depth, in	Volume, in^3	Normal	Tangential	Width, in	Depth, in	Volume in^3
	Jasper quartzite					Dresser basalt				
1	4,223	227	0.20	0.031	0.046	4,025	89	0.14	0.017	0.015
2	7,241	535	.39	.065	.167	5,103	312	.35	.042	.098
3	9,252	800	.49	.080	.317	5,952	449	.38	.053	.163
4	11,412	1,119	.67	.109	.502	6.966	553	.41	.062	.216
5	13,566	1,435	.82	.137	.850	7.863	710	.47	.067	.289
6	14,632	1,809	.90	.150	.155	8,694	924	.67	.094	.515
7	12,298	1,186	.70	.115	.569	9,366	1,038	.68	.100	.576
8	10,184	784	.51	.088	.355	11,278	1,343	.70	.114	.714
9	8,060	553	.45	.074	.251	10,107	1,085	.70	.103	.528
10	6,094	301	.30	.055	.118	12,169	1,531	.87	.122	.924
11	4,934	181	.21	.042	.067	12,978	1,736	1.03	.140	1.093
12	10,219	853	.55	.094	.403	14,049	2,057	1.11	.151	1.525
13	7,974	555	.42	.072	.214	5,039	235	.23	.028	.076
14	4,261	110	.16	.030	.034	6,006	396	.30	.046	.164
15	5,111	179	.20	.038	.064	7,075	571	.44	.059	.248
16	6,026	264	.27	.051	.108	8,008	758	.57	.077	.351
17	7,256	399	.35	.059	.163	10,140	1,206	.72	.102	.652
18	9,191	590	.44	.083	.314	11,020	1,318	.76	.115	.754
19	11,200	1,027	.57	.114	.477	12,048	608	.82	.118	.775
20	12,185	1,201	.71	.112	.736	4,933	246	.23	.036	.071
21	13,091	1,416	.75	.124	.809	13,187	1,771	.93	.148	1.036
22	14,230	1,579	.88	.140	.975	14,130	1,880	1.07	.156	1.357
23	14,512	1,725	.91	.150	1.082	7,012	553	.42	.079	.252
24	13,377	1,403	.81	.131	.780	9,039	868	.57	.127	.399
25	7,180	344	.27	.054	.126	11,145	1.243	.89	.189	.793
26	6,217	320	.28	.048	.119	13,118	1,825	1.08	.237	1.403
27	4,075	98	.17	.030	.031	13,996	1,964	1.03	.157	1.419
28	5,001	169	.34	.039	.065	-	-	-	-	-
29	8,025	504	.45	.073	.236	-	-	-	-	-
30	9,016	595	.48	.082	.278	-	-	-	-	-
31	10,118	760	.56	.088	.370	-	-	-	-	-
32	11,176	1,021	.79	.109	.607	-	-	-	-	-
33	12,380	1,193	.71	.126	.664	-	-	-	-	-
34	13,258	1,433	.90	.139	.996	-	-	-	-	-
35	12,235	1,057	.69	.116	.590	-	-	-	-	-
36	10,039	684	.49	.085	.303	-	-	-	-	-
37	7,882	474	.41	.068	.189	-	-	-	-	-
38	5,968	271	.26	.048	.088	-	-	-	-	-
39	5,260	207	.23	.045	.083	-	-	-	-	-
40	3,907	92	.15	.031	.034	-	-	-	-	-
41	6,900	362	.29	.058	.139	-	-	-	-	-

☆ U. S. GOVERNMENT PRINTING OFFICE: 1974-605-663/516

INT.-BU.OF MINES,PGH.,PA. 19600